ON CONFIGURATIONS OF SPATIAL PLANAR GRAPHS

A Dissertation

Presented to the Faculty of the Graduate School

of Cornell University

in Partial Fulfillment of the Requirements for the Degree of

Doctor of Philosophy

by

Andrew Len Marshall

August 2014

ON CONFIGURATIONS OF SPATIAL PLANAR GRAPHS

Andrew Len Marshall, Ph.D.

Cornell University 2014

We investigate the homotopy type of a variety of families of configurations of graphs in $\mathbb{R}^3$ and S^3. Preliminary results give that the linear configurations of the tetrahedral graph in $\mathbb{R}^3$ has the homotopy type of the double mapping cylinder $SO(3)/A_4 \leftarrow SO(3)/A_3 \rightarrow SO(3)/S_3$, for A_n the alternating group and S_n the symmetric group. Two presentations and an action on the free group are given. This result is generalized to two families of configuration spaces of codimension 2 and 3 skeleta of simplices in $\mathbb{R}^n$. The final segment is toward understanding the space of unknotted smooth embeddings of spatial planar graphs.

BIOGRAPHICAL SKETCH

Andrew Len Stephens Marshall was born to parents Charles David Marshall and Elizabeth Dale Marshall on September 12th, 1977, in Ogdensburg New York. From 1977-1991 he lived with his older brother Nicholas Armstrong Marshall (1975-) and parents in Potsdam New York. After moving to Lawrence Kansas in 1991 and humoring high school for 2 years, Andrew opted instead for touring the U.S. via freight train, educating himself in music, travel, society and entertainment from 1994-2000. Andrew Marshall is father to Electra Bella Marshall, born in Cork, Ireland on the 11th of March, 2002 and Roman Taghg Marshall, born in Cork, Ireland on the 16th of August, 2003. He holds a Bachelors of Arts degree in mathematics from the University of Santa Cruz, California where he graduated with highest honors in 2007, and a Masters of Science in mathematics from Cornell University in 2011.

This document is dedicated to all those who work toward a sanctuary of mind, for the sake of play.

ACKNOWLEDGEMENTS

I would like to acknowledge, primarily, my adviser. I am sure that ego plays some part in the success of the more powerful mathematicians, of which I include Allen Hatcher, and yet I have not met a more humble and patient mathematician. This paradox has provided me the ideal environment in which to grow: both a source for knowledge and insight and a patient ear for my thoughts and foibles. I am indebted for many hours of conversation and a good portion of the (better) ideas contained herein.

My father, Charles Marshall, knows he played an absolutely crucial role in my accomplishments here. Were it not for he, I would be perhaps more peaceful, certainly more docile; less opinionated and far less troubled. I love him dearly for his love of mathematics and mind, for his integrity and for his intensity.

My children, Roman and Electra: I owe so much to you. You are on my mind always. Before you learned to understand, you laughed at my jokes. Before you knew jokes, you made me laugh. I love you both dearly.

For friendly conversations that have been mathematically insightful, I have to thank Jimmy Mathews, Lucien Clavier, Amin Saied and Dominic Dotterrer. I have met too many wonderful people, influential in my life, to list here. To be brief: My brother Nick, dear blood, trouble maker, thank you for being a best friend so often. Gaby Wolodarski, Tom Birt, Richard Robinson, Edward Small, Laura Escobar Vega, Aleks Sedriks, Destiny Shelton, Alan Blank, Robert Pettit, Peter Luthy, Kelly Cook, Kelsey Houston-Edwards, Paul Brooks, Mark Cerenzia, Maus, Nadia Rodriguez: some favorite people are necessary, everyone knows that! I owe a special gratitude to Jason Anema, who has been a dear friend for all my years here, through many great and many trying times. I consider you family and will

continue to do so.

I would like to thank Ken Brown and Tim Riley both for their kindness and their support on my committee. In particular, Tim Riley's suggestions have been very helpful. I would also like to thank Maria Tarrell and Laurent Saloff-Coste for supporting me as an educator; it is a responsibility I take very seriously.

Lastly, and certainly not least of all, I would like to acknowledge William Thurston along with the other 20th century giants, notably Henri Poincaré, René Thom and Alexander Grothendieck, who dared to philosophize, to wax poetic, to talk of *how* mathematics is done, and who built bridges out of mathematics to the outside world of mind. May we all, at the risk of sloppiness, hazard nonsense and follow suit, for the enrichment of our own lives.

TABLE OF CONTENTS

LIST OF FIGURES

CHAPTER 1

INTRODUCTION AND DEFINITIONS

1.1 Introduction

Configuration spaces are as ubiquitous in topology as one cares to emphasize. Indeed the chief merit of a mathematical space is how it parametrizes various families of objects. The Möbius strip, for example, is a delightful curio in its own right, but asserts its practicality in any context where a set of two distinct indistinguishable values on a circle are relevant. And so points in a low dimensional space make up the first non-trivial configuration spaces and are implicit in much of physics dating back before Poincaré's famous solution to the n-body problem which begat chaos [23].

Braid groups are some of the earliest algebraic topological artifacts to come from configuration spaces, as they are the fundamental groups of configurations of indistinguishable points in a plane, the study of which dates to Artin's explicit introduction and before that to late 19th century work of Hurwitz (see [3], [16]). Braid groups have enjoyed enormous attention across group theory, representation theory, category theory, cryptography, topology, physics, robotics, chemistry, etc. The references abound. The inquiry into embeddings of X into Y modulo either automorphisms of X or (slightly more generally) images of X gives rise to a wealth of generalizations. Braids on surfaces have been studied extensively (see [1], [2], [18]) and braids on graphs have been studied (see [9], [22]). A remarkable

recent theorem on manifold braids states that there are lens spaces (certain quotients of S^3 by finite cyclic groups) which are homotopy equivalent but which have homotopically distinct configuration spaces ([14]).

The present volume concerns configuration spaces of graphs in $\mathbb{R}^3$ and S^3, which are called *spatial graphs* (this may refer to either embeddings or configurations), of which much is known. In particular, the set of components of such spaces are a natural generalization of knot theory (see [20], [21]). These components will not be investigated herein, but only the component containing the embeddings which place the graph in a plane in $\mathbb{R}^3$.

The braid group acts, via isotopies of distinct indistinguishable points in the plane, on the fundamental group of the complement of a configuration and is realized, from this picture, as a subgoup of the automorphisms of the free group. Specifically loops in $\pi_1(C_n(\mathbb{R}^2))$ act on the fundamental group F_n of the complement of a configuration. This relationship was generalized to configurations of unlinked, unknotted C^∞ circles in $\mathbb{R}^3$ in the thesis *A Generalization of Braid Theory* of Dahm [8], and the homotopy type of the space of C^∞-embedded, unlinked circles was described in [5], which generalized Smale's conjecture that the space of unknotted smoothly embeddings of a circle in $\mathbb{R}^3$ deformation retracts to the round unit circles, proved in [10]. A tetrahedral graph linearly embedded in $\mathbb{R}^3$ also has the property that its complement has a free fundamental group F_3, so that the fundamental group of the space of linear configurations of a tetrahedral graph in $\mathbb{R}^3$ maps to a subgroup of $Aut(F_3)$. Two presentations are given in Section 2.4.

The unifying theme throughout this thesis is to prove results about the topology of configuration spaces of a well-behaved family of graphs in ambient $\mathbb{R}^3$. Whenever

possible, the family is extended to allow for the widest range of results following each development.

In the linear case (chapters 2-4) this amounts to describing the homotopy type of configuration spaces of linearly embedded complete graphs K_4 and K_5 in $\mathbb{R}^3$; in showing these are homotopy equivalent; in giving two natural presentations of $\pi_1(C_L(K_4, \mathbb{R}^3))$; in presenting the subgroup of $Aut(F_3)$ resulting from the action of $\pi_1(C_L(K_4, \mathbb{R}^3))$ on $\pi_1(\mathbb{R}^3 \setminus K_4)$; and in generalizing the homotopy equivalence between the two spaces to the families $C_L((\Delta^n)^{n-2}, \mathbb{R}^n)$ and $C_L((\Delta^{n+1})^{n-2}, \mathbb{R}^n)$, of codimension 2 and 3 (respectively) skeleta of simplices linearly embedded in $\mathbb{R}^n$ (i.e., they are homotopy equivalent for each n). The fundamental groups of these spaces can be derived from the construction, and are analogous to the $n = 3$ case, in an obvious way. The actions on the fundamental groups of the complements should be obvious from the construction given, as well, though not explicitly given here.

The main machinery for these linear cases is Radon's Theorem (see [19]), which limits the kinds of degeneracies which can occur; an $O(n)$-equivariant Gram-Schmidt process that is readily gleaned from the polar decomposition of $GL(n)$, used to linearly deformation retract $GL(n)$ to $O(n)$ and modified to deformation retract the space of simplices to the space of regular simplices; and 2 original gluing arguments to reduce the problem to an application of Van Kampen's Theorem.

In the C^∞ case (Chapter 5), "simple results with all viable generalizations" means nearly computing the homotopy type of the "base" component (viz. unknotted) of polyhedral trivalent graphs (of which K_4 is the most basic). Generalizing from trivalent to higher valences is made possible via [4]. Work is on-going (by

this author) to generalize to the full planar case (again, and always: unknotted), although that work has not made it into the present volume.

The machinery used here is chiefly Smale's Conjecture $\mathrm{Diff}(S^3) \simeq \mathrm{PL}(S^3) \simeq O(4)$, applied in a few different forms, all proved in [10], although the results here also rely on work from the 80's and 90's on spatial graphs [viz. Boyle, Kauffman, Taniyama, et al.].

1.2 Outline

In Chapter 2, Sections 2.1-2.3, we investigate the homotopy type of the space $C(K_4) = Emb(K_4, \mathbb{R}^3)/S_4$, where K_4 is the tetrahedral graph (which on occasion will be referred to as $(\Delta^3)^1$, the 1-skeleton of the 3-simplex), and C, Emb denote linear configurations, linear embeddings, respectively. Here, S_4 is the symmetric group on 4 elements, a *configuration* is the image of an embedding, and an embedding is *linear* if it is affine linear when restricted to each edge. We will sometimes refer to a tetrahedral graph as a tetrahedron, even when it is planar, by a convenient abuse of terminology.

Section 2.4 gives a presentation of $\pi_1(C(K_4))$ in terms of a set of generators on which the automorphism group $Aut(\pi_1(C(K_4)))$ acts transitively, and this presentation is related to that given by the amalgamated free product obtained from the Van Kampen decomposition of the space.

Section 2.5 is a brief look at the action on the fundamental group F_3 of the complement of a configuration.

Chapter 3 introduces a higher dimensional analog where now we consider the $(n-2)$-skeleton of the n-simplex linearly embedded in $\mathbb{R}^n$. The result of this section is that this space has the homotopy type of the double mapping cylinder

$$SO(n)/A_{n+1} \leftarrow SO(n)/A_n \rightarrow SO(n)/S_n,$$

where A_n and S_n are alternating and symmetric groups, respectively and the maps are those surjections induced by the inclusions of A_n in A_{n+1} and S_n, respectively.

Chapter 4 considers the case from Chapter 3, but where we've increased the number of vertices by 1, while keeping the same dimension skeleton and ambient space. The main result of this chapter is that this configuration space is homotopy equivalent to the previous one.

We note that the homotopy equivalence of chapter 4 does not hold when we increase the simplex dimension again. For example, configurations of $K_6 = (\Delta^5)^1$ linearly embedded in $\mathbb{R}^3$ can contain 1 or 3 Hopf links depending on whether they contain a trefoil or not (see [12]), so this configuration space is not connected. Nor does the homotopy equivalence hold for the case $n = 2$, where the respective spaces are $C_3(\mathbb{R}^2)$ and $C_4(\mathbb{R}^2)$ (configurations of 3 and 4 points in the plane, respectively). Here, the skeleton of the simplex is not connected so the generalization given of the non-planarity of K_5 does not apply (as evidenced by the fact that $(\Delta^3)^0$ embeds in a 1-dimensional space) and the symmetry is different since for a square configuration of points, the diagonals are interchangeable (i.e., the Radon point doesn't distinguish a particular edge, as it does when $n > 2$). This case is well-understood, as it gives Eilenberg-MacLane spaces for the braid group on 3 and 4 strands, respectively.

In Chapter 5 we consider the C^∞ planar embeddings of a trivalent polyhedral graph X^1 in $\mathbb{R}^3$. Here we use two fibrations, the Smale Conjecture, and some geometry to conclude with the theorem

$$Emb_0(X^1, \mathbb{R}^3) \simeq \bigvee^n S^1 \times SO(3),$$

where Emb_0 is the component of the smooth embedding space which contains the planar graphs.

CHAPTER 2

THE LINEAR TETRAHEDRAL GRAPH

2.1 Space of Embeddings

The space $\widetilde{C(K_4)} = Emb(K_4, \mathbb{R}^3) \subset \mathbb{R}^{12}$ is precisely those ordered 4-tuples of points in $\mathbb{R}^3$ such that if all four points are coplanar, then one is in the interior of the triangle formed by the other three (note that this excludes the special cases of 3 collinear points or 2 coincidental points). The action of S_4 on $\widetilde{C(K_4)}$ gives a covering map to our space of interest, $C(K_4)$. The homotopy type of the covering space is given by our first theorem.

Theorem 2.1.1. *The space $\widetilde{C(K_4)}$ of linear embeddings of the tetrahedral graph into $\mathbb{R}^3$ is homotopy equivalent to $(\bigvee^3 S^1) \times \mathrm{SO}(3)$.*

Proof. The space $\widetilde{C(K_4)}$ can be seen as a fiber bundle of possible positions for the fourth point over the space $Emb(K_3, \mathbb{R}^3)$ of labeled triangles in $\mathbb{R}^3$, where $Emb(K_3, \mathbb{R}^3)$ parametrizes the locations of the first three points. Fixing some triangle $b \in Emb(K_3, \mathbb{R}^3)$ we see that the fourth point can be either outside of the plane spanned by b or within that plane, either interior to b or interior to one of the three cones extending the edges of b (see figure 2.1).

The fiber over the fixed base point b is thus seen to deformation retract to a wedge of three circles (see figure 2.2).

Furthermore, for an arbitrary fiber F_b, there is a unique orientation preserving affine linear transformation T taking the triangle $b = \text{convex span}(b_0, b_1, b_2)$ to the

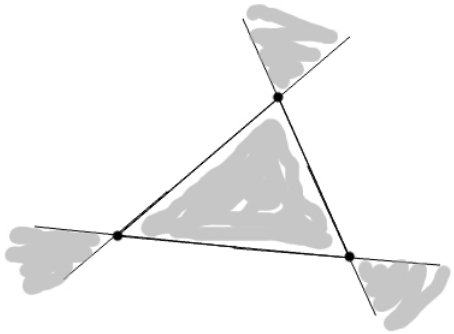

Figure 2.1: The four regions a fourth point can occupy in the plane containing the other three, while still forming an embedded K_4.

standard labeled triangle c, defined by $c_0 = (0,0,0),\ c_1 = (1,0,0),\ c_2 = (0,1,0)$, such that $T(b_i) = c_i$ and $T(b_0 + (b_1 - b_0) \times (b_2 - b_0)) = (0,0,1)$ (see figure 2.3). The map T, when restricted to a fiber, is a homeomorphism to the "typical" fiber F_c and varies continuously as the base point varies, thus the fiber bundle is trivial.

Finally, the base space of labeled triangles in $\mathbb{R}^3$ is homotopy equivalent to $SO(3)$, as is easily seen by regarding a labeled triangle $b = \text{convex span}(b_0, b_1, b_2)$ as a basis $((b_1 - b_0), (b_2 - b_0), (b_1 - b_0) \times (b_2 - b_0))$ and applying the Gram-Schmidt deformation retraction while translating to the origin. □

2.2 Space of Pyramids

A reasonable (i.e., compact, low-dimensional) model of $C(K_4)$ is the subset of tetrahedral graphs having 3-fold symmetry. We call these *pyramids*, and denote the space by $\mathcal{P}$. Specifically, $\mathcal{P}$ will be those tetrahedra with 3 unit length edges and 3 edges of length $\ell \in [3^{-1/2}, 1]$, with barycenter at the origin. Those with

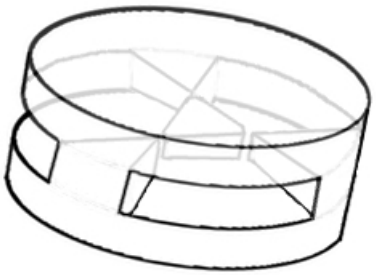

Figure 2.2: We remove a thickening of the planar subset of $\mathbb{R}^3$ where the fourth point would force an intersection of edges, leaving a space homotopy equivalent to $\bigvee^3 S^1$.

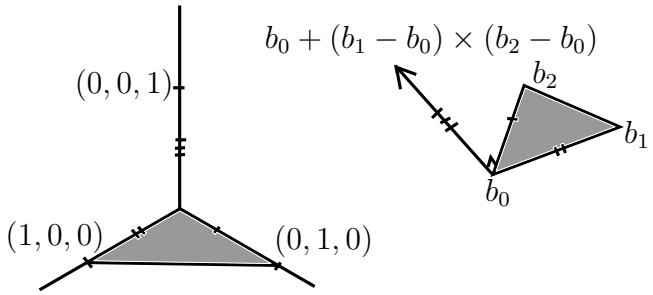

Figure 2.3: The map T is defined by its action on b, which it sends to c, along with the specific extension sending $b_0 + (b_1 - b_0) \times (b_2 - b_0)$ to $(0,0,1)$.

$\ell = 1$ are denoted $\mathcal{R}$, for regular; those with $\ell = 3^{-1/2}$ are denoted $\mathcal{F}$, for flat.

The unlabeled pyramid space $\mathcal{P}$ is covered by the space $\widetilde{\mathcal{P}}$ of labeled pyramids, labeled with vertices v_i, $1 \leq ile4$. From $\widetilde{\mathcal{P}}$, we have a map which forgets the 4th point v_4 and maps the isosceles triangle of v_1, v_2, v_3 to the equilateral labeled triangle centered at the origin, by normalizing the altitude in the direction of the apex. The space of unit edge labeled isosceles triangles centered at the origin is parametrized by $SO(3)$.

Fixing a labeled triangle b in the image of this map, we see that b is mapped to by a set of tetrahedra parametrized by the graph which is the suspension of 4 points, homotopically equivalent to a wedge of 3 circles. Specifically, the fourth point can make up a pyramid with b as its base, for which there is a line segment's worth of choices, or the given base b can be the image of a pyramid with the isosceles face v_1, v_2, v_3 parallel to the plane containing b. For each of $i = 1, 2, 3$ there is an arc of pyramids with apex v_i of the isosceles face v_1, v_2, v_3, so the preimage of a point is the graph with 4 edges, 2 vertices and no edges which are loops. There are local trivializations, which makes this map a fiber bundle, but in fact there is a global trivialization as the next theorem asserts.

Theorem 2.2.1. *The space $\widetilde{\mathcal{P}}$ of labeled pyramids in $\mathbb{R}^3$ is homeomorphic to $(\bigvee^3 S^1) \times \mathrm{SO}(3)$.*

Proof. The map from $\widetilde{\mathcal{P}}$ to $SO(3)$ is given above. The map to the suspension of 4 points is given by mapping the pyramid to the edge with the same label as the apex vertex of the pyramid (i.e., vertex v_4). This edge is parametrized by the height of the apex. The edges of the graph are oriented, since for labeled triangles in $\mathbb{R}^3$ there is a well-defined positive normal direction, so that heights vary in $[-3^{-1/2}, 3^{-1/2}]$. The vertices of the graph correspond to the two components of regular labeled tetrahedra. (See figure 2.4).

□

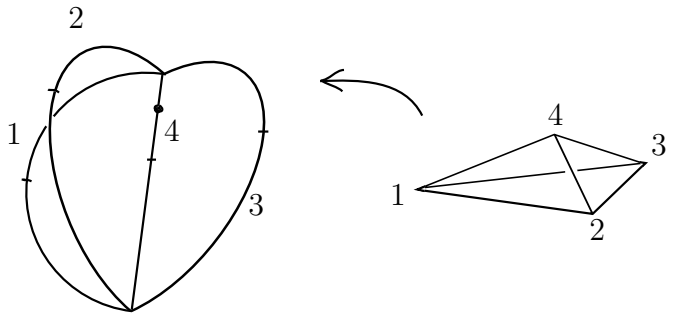

Figure 2.4: The map from $\widetilde{\mathcal{P}}$ to the suspension of 4 points. Each labeled edge corresponds to the various heights for the corresponding apex vertex.

2.3 Explicit Deformation Retraction from $C(K_4)$ to $\mathcal{P}$

In this chapter we give an explicit deformation retraction from $C(K_4)$ to $\mathcal{P}$. We begin with the regularization of non-degenerate tetrahedra.

We will require a signed-permutation-equivariant version of the Gram Schmidt process. For the sake of an explicit deformation retraction we use the method called Löwdin orthogonalization which is as follows (the original reference is here [15]). To each basis of $\mathbb{R}^3$ given as columns of the matrix B define a path $p_B(t) = (1-t)B + tB(B^TB)^{-1/2}$. The terminal point is B times the inverse of the positive square root of the matrix B^TB, which is a positive definite symmetric matrix. (Polar decomposition gives $B = OS$, where $O \in O(3)$ and $S = S^T$. Here O is the terminal point and S is $(B^TB)^{1/2}$) Multiplying this terminal point by its transpose, we have

$$\begin{aligned}(B(B^TB)^{-1/2}) \cdot (B(B^TB)^{-1/2})^T &= B(B^TB)^{-1/2}(B^TB)^{-1/2}B^T \\ &= BB^{-1}(B^T)^{-1}B^T = I,\end{aligned}$$

so that $B(B^TB)^{-1/2}$ is orthogonal.

If we left act on $\mathbb{R}^{3\times 3}$ by the linear transformation B^{-1} we get $B^{-1}p_B(t) = (1-t)I + t(B^TB)^{-1/2}$ which is a convex combination of two positive definite symmetric matrices for each $t \in [0,1]$, so in particular it is invertible. Hence p is a path in $GL(3)$ which terminates in $O(3)$. As we change B continuously, p_B changes continuously, so in fact we have a deformation retraction from $GL(3)$ to $O(3)$. Finally, let $P \in \mathbb{Z}_2 \wr S_3$ be a signed permutation matrix (i.e., a matrix with exactly one non-zero element valued in $\{\pm 1\}$ in each row and column). Then from BP the defined path is

$$\begin{aligned} p_{BP}(t) &= (1-t)BP + tBP((BP)^TBP)^{-1/2} \\ &= (1-t)BP + tBPP^T(B^TB)^{-1/2}P \\ &= ((1-t)B + tB(B^TB)^{-1/2}) \cdot P = p_B(t)P \end{aligned}$$

so that the deformation retraction is equivariant with respect to the right $\mathbb{Z}_2 \wr S_3$ action. (Note, in fact, the same calculation shows equivariance for $O(3)$.)

Theorem 2.3.1. *The space of (non-degenerate) tetrahedra in $\mathbb{R}^3$ deformation retracts to $\mathcal{R}$, the space of regular tetrahedra in $\mathbb{R}^3$.*

Proof. To each tetrahedron we assign what we will call its *bimedian basis* which is the (unordered) collection of 3 line segments joining midpoints of opposite (necessarily skew) edges (see figure 2.5). These line segments intersect at the barycenter, which bisects each line segment. It is easy to verify that E the *standard bimedian basis*—i.e., the basis formed by the standard basis vectors and their negations—has exactly 2 tetrahedra which have E for a bimedian basis, which differ by the reflection $-I$. Any other bimedian basis is then the image of this one under an invertible linear map (modulo translation, which we are not concerned with), so that the space of tetrahedra is a double cover of the space of bimedian bases. Any

deformation retraction of $GL(3)$ to $O(3)$ which is $\mathbb{Z}_2 \wr S_3$-equivariant descends to a deformation retraction of bimedian bases to the *orthonormal bimedian bases*, which then lifts to the double cover, resulting in regular tetrahedra. Thus the Löwdin process gives a regularization of tetrahedra in $\mathbb{R}^3$. □

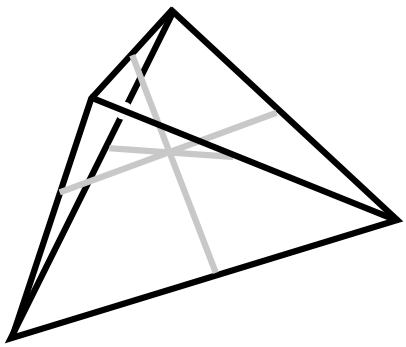

Figure 2.5: The bimedian basis of a tetrahedron is shown in gray.

As a side remark, the set of determinant 0 matrices in $\mathbb{R}^{n\times n}$ is in fact the cut locus of $O(n)$ under the Frobenius (i.e., Euclidean) norm, meaning the points in $\mathbb{R}^{n\times n}$ which have a unique nearest $O(n)$ element are precisely $GL(n)$. For general n, the Löwdin orthogonalization achieves the minimizing geodesic from $GL(n)$ to $O(n)$. (We omit the easy calculations showing this.) However, the method of picking a bimedian basis and thus lifting orthogonalization of a bases to regularization of a simplex does not generalize to arbitrary n. We require a homomorphism from S_{n+1}, the symmetries of the n-simplex, to $\mathbb{Z}_2 \wr S_n$, the symmetries of the bimedian basis. The image of this homomorphism must at least generate $S_n < \mathbb{Z}_2 \wr S_n$, and so must be injective for $n > 3$, since S_{n+1}'s only normal subgoup is A_{n+1}. The respective orders are $(n+1)!$ and $2^n n!$, thus such a method can only exist when $n = 2^k - 1$ for some k. In chapter 3 and 4 we provide two more deformation retractions, which will generalize to similar cases in higher dimensions.

We now use the Löwdin regularization of non-degenerate tetrahedra to deformation retract all of $C(K_4)$ to $\mathcal{P}$.

Theorem 2.3.2. *There is a deformation retraction from $C(K_4)$ to $\mathcal{P}$, the space of pyramids.*

Proof. In $C(K_4)$ we have planar tetrahedra for which we define the non-extremal vertex to have solid angle of 2π (this is the continuous extension of the solid angle function), but none with all solid angles 0, though we can decrease the maximum solid angle to any small $\epsilon > 0$, by approaching a planar quadrilateral graph with intersecting diagonals. We thus have a surjective function which gives the maximum solid angle

$$\alpha : C(K_4) \to (0, 2\pi].$$

The sum of solid angles is in fact bounded above by 2π (see Lemma 3.3.1) so that any tetrahedron $x \in \alpha^{-1}(\pi, 2\pi]$ has a vertex of uniquely greatest solid angle. For these tetrahedra, call the face opposite this vertex the *wide face* W_x, and call the line perpendicular to the wide face at the barycenter of the wide face $W_x^{\perp}$. For tetrahedra in $\alpha^{-1}(\pi, 2\pi)$ any deformation retraction Φ_t defines a map $\phi_x : I \to \mathrm{Aff}(\mathbb{R}^3)$, from the interval to affine transformations of $\mathbb{R}^3$, which sends a time t to the transformation which takes W_x to $\Phi_t(W_x)$ and which takes $W_x^{\perp}$ to $\Phi_t(W_x)^{\perp}$, preserving distance and orientation. Let η be defined on tetrahedra in $\alpha^{-1}(\pi, 2\pi]$ as the reparametrization $\eta(x) = \alpha(x)/\pi - 1$, so that going from regular to degenerate, $1 - \eta(x)$ ranges from 1 to 0 (see fig 2.6)). Note, for ease of understanding where this argument is going, that $(\phi_x(t)^{-1} \circ \Phi_t)(x)$ is a path from x, which keeps W_x fixed and ends in being height $\sqrt{2/3}$ above W_x, directly over its barycenter. We will use the solid angle of a vertex which is near its opposite

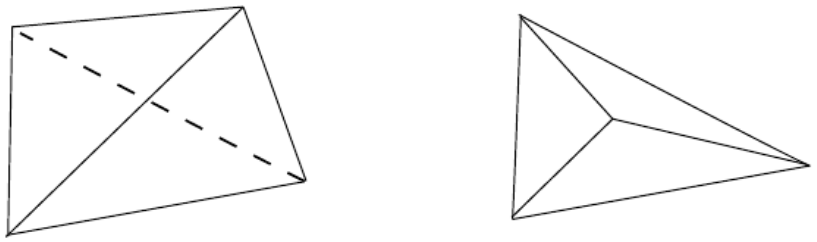

Figure 2.6: The parameter η varies from 0 (left) to 1 (right).

face W_x as a parameter to slow down the motion of W_x, so that in the limiting case of the degenerate tetrahedron, the extremal triangle will be fixed.

Let ψ_t be defined on $\alpha^{-1}(\pi, 2\pi)$ as scaling by a factor of $1 - \eta(x)$ along $W^{\perp}_{\Phi_t(x)}$ followed by $(\phi_x(\eta(x)t))^{-1}$, and extended to $\alpha^{-1}(0, 2\pi]$ by declaring $\psi_t|_{\alpha^{-1}(0,\pi]} \equiv \mathrm{id}$. Consider the deformation retraction

$$\Psi_t = \psi_t \circ \Phi_t$$

where Φ_t is the deformation retraction given by the Löwdin orthogonalization above. The picture is this: as our tetrahedron approaches being degenerate, $1 - \eta$ approaches 0 and this parameter is used to scale the result of the regularization by Φ_t, to be a pyramid which becomes flatter as the greatest solid angle becomes greater. The same parameter is used to undo some portion of how Φ_x moves W_x. In the limit $\eta \to 1$ the wide face is fixed under Ψ_t (see figure 2.7).

Note that because Φ_t sends vertices along constant velocity paths, so does Ψ_t. Then we can extend Φ_t to $\alpha^{-1}(2\pi)$ by moving the interior vertex v along the straight-line path to the barycenter of W_x, while keeping W_x fixed. This path is the limit of the straight-line paths taken by vertices of large solid angle vertex v_t which approach v, by construction of the deformation retraction. Finally, we

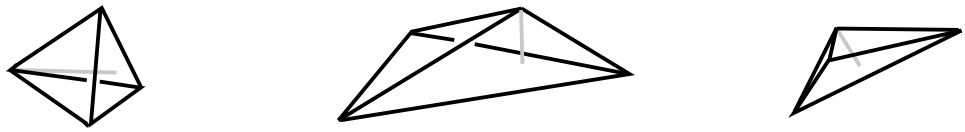

Figure 2.7: The solid angle opposite its wide face is used both to scale down the resulting regular tetrahedron and impede the motion of the wide face.

equilateralize the wide face while the vertex opposite is kept over the barycenter of the wide face by–extending isometrically in the perpendicular direction again–some choice of deformation retraction which equilateralizes (and normalizes the length of) triangles. The image of the deformation retraction is the space of pyramids, $\mathcal{P}$, and these are stationary under the deformation retraction. □

This technique will be revisited in Chapter 3. We give it the name *damping*, as α is used to impede the motion of the wide face under Φ_t.

2.4 Presentations

Section 2.3 gave $\mathcal{P}$ as a low-dimensional, compact model of $C(K_4)$. This model reveals the fundamental group, by the application of van Kampen's Theorem. Specifically, divide $\mathcal{P}$ into closed subsets U, of those with altitudes $a \geq \frac{1}{2}\sqrt{\frac{2}{3}}$ (half the height of a regular, unit edge tetrahedron), and V, with altitudes $a \leq \frac{1}{2}\sqrt{\frac{2}{3}}$. The first clearly deformation retracts to $\mathcal{R}$, the regular tetrahedra, and the second to $\mathcal{F}$, the planar pyramids. The intersection $U \cap V$ of half-high pyramids is a neighborhood retract of $\mathcal{P}$, as is required for van Kampen's theorem, and has as fundamental group $2A_3 \cong \mathbb{Z}_6$, the binary double cover of 3-fold symmetry in

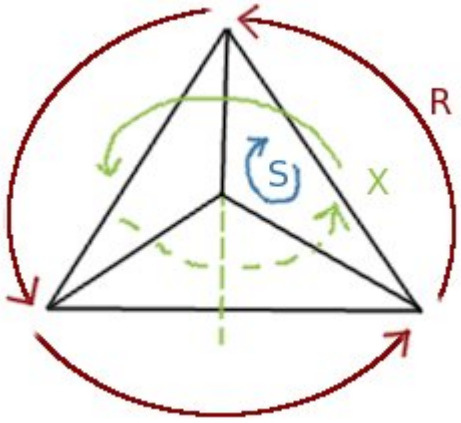

Figure 2.8: The generators X, R, S. We consider R, S rigid motions of the regular tetrahedron, while considering X a rotation of π of the planar tetrahedron.

$\mathbb{R}^3$ coming from lifting $A_3 < SO(3)$ to the double cover S^3. The symmetries of the regular tetrahedron sitting in $\mathbb{R}^3$ form a copy of A_4 inside $SO(3)$ (i.e., even permutations are identified with orientation preserving symmetries of the tetrahedron), so that $\pi_1(U) \cong \pi_1(\mathcal{R}) \cong 2A_4$, the double cover of A_4 by a subgroup of S^3. The symmetries of the equilateral triangle form a copy of $Dih_3 < SO(3)$, so that $\pi_1(V) \cong \pi_1(\mathcal{F}) \cong Dic_3$, the dicyclic group of order 12 (defined, for example, by the relations $\langle R, X \mid R^6 = 1,\ X^2 = R^3,\ X^{-1}RX = R^{-1}\rangle$). Thus, from van Kampen's Theorem, we have

Theorem 2.4.1. *The fundamental group of $C(K_4)$ is*

$$2A_4 *_{2A_3} Dic_3 \cong \langle X, R, S \mid X^2 = R^3 = S^3 = (SR)^3,\ XR = R^{-1}X\rangle.$$

Here X is the rotation of order 4 in $\pi_1(\mathcal{P})$ which reflects the planar tetrahedron (by a rotation of π in a given direction), and R, S are two face rotations as given in figure 2.8.

Proof. Given the above decomposition of pyramids, van Kampen's theorem gives that the fundamental group is the amalgamated product of the binary tetrahedral group and the dicyclic group of order 12, amalgamated along a cyclic group of order 6. A generator for the latter is a rotation of the half-high pyramid $2\pi/3$, which is denoted R. The dicyclic group, as it appears here, is generated by R (i.e., rotating the triangle) and a rotation of the triangle $\pi/2$ about a line coplanar with the triangle which bisects one angle, and has a presentation given on the previous page. The binary tetrahedral group is generated by R and another rotation about an altitude, which we've denoted S, and has a presentation $\langle S, R \mid (SR)^2 = S^3 = R^3 \rangle$. □

Another presentation of $\pi_1(C(K_4))$ is given in terms of loops from a base point in $\mathcal{F}$ which transpose the center vertex and an extremal vertex by passing the center vertex up and over while passing the extremal vertex down and under. (Figure 2.9 shows such a generator.) This presentation has two advantages. First, it is particularly simple and is symmetric, in the sense that $Aut(\pi_1(C(K_4)))$ acts transitively on it. Second, it makes transparent the action of $\pi_1(C(K_4))$ on the free group on three generators F_3, the fundamental group of the complement of a given configuration, as section 2.5 explains.

Theorem 2.4.2. *The fundamental group of $C(K_4)$ is generated by three elements*

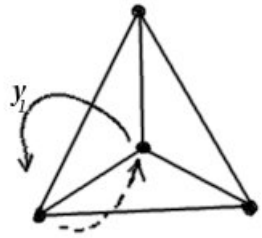

Figure 2.9: The generator y_1 which transposes the center vertex with the one in position 1, by passing the center up and over while passing the extremal vertex down and under.

$\{y_1, y_2, y_3\}$, *subject to the following relations.*

$$(y_j y_i^{-1})^3 = (y_k y_l^{-1})^3 \text{ for neither side trivial,} \tag{i}$$

$$y_i y_j^{-1} y_i = y_j^{-1} y_i y_j^{-1} \text{ for } i \neq j, \tag{ii}$$

$$y_k y_j^{-1} y_i y_j^{-1} y_k = y_j^{-1} y_i y_j^{-1} \text{ for } i, j, k \text{ distinct.} \tag{iii}$$

The isomorphism can be seen by observing one presentation in terms of the geometry of the other, the fine details of which we omit. The map is given by the identities

$$\begin{array}{rclcrcl} S & = & y_3^{-1} y_2 & & y_3 & = & X^{-1} S R^{-1} S^{-1} \\ R & = & y_2^{-1} y_3 y_1^{-1} y_2 & \text{and} & y_2 & = & R X^{-1} S R^{-1} S^{-1} R^{-1} \\ X & = & y_3^{-1} y_1 y_3^{-1} & & y_1 & = & R^{-1} X^{-1} S R^{-1} S^{-1} R. \end{array}$$

In terms of these generators, the kernel $F_3 \times \mathbb{Z}_2$ of the map $\pi_1(C(K_4)) \to S_4$ is generated by each of the three y_i^2, for the left factor, and $\tau = (y_i y_j^{-1})^3$ (any two distinct i, j), for the right factor. Geometrically, this can be seen by viewing $y_i y_j^{-1}$ as a rotation of the tetrahedron by $2\pi/3$ so that it cubes to a rotation of 2π, which explains the first set of relations (i). The second set of relations (ii) can be

rewritten, by multiplying both sides by the left side, to state that $y_i y_j^{-1} y_i$ squares to τ. Geometrically this is so, because $y_i y_j^{-1} y_i$ is effectively a rotation of π about the edge e_k which would get reversed by y_k (see figure 2.10). The third set of relations (iii) can then be rewritten to state that conjugation of y_k by this particular square root of τ inverts y_k. This is easily seen from the fact that the circle along which the end points of e_k travel under the action of y_k gets reversed in orientation by $y_i y_j^{-1} y_i$. It should be remarked that τ is thus central, as it commutes with y_k, for any k. Also, we note from (i) that $(y_i y_j^{-1})^3 = (y_j y_i^{-1})^3$ so that $(y_i y_j^{-1})^6 = \tau^2 = 1$.

It is worth noting that the families (i),(ii) and (iii) of relations above are independent in the sense that no two families generate the third. Without relation (iii) the quotient by the subgroup generated by $\{y_i^2\}$, $i = 1, 2, 3$, and $(y_i y_j)^3$ has the Cayley graph of figure 2.11. In particular, it is not finite and so is not S_4, thus (iii) is independent. Restricting to a subgroup generated by two generators y_i, y_j renders (iii) inconsequential, and gives $(y_i y_j^{-1})^3 = (y_j y_i^{-1})^3$ as the only consequence of (i), so that it's easy to see (by a change of basis $h = y_i, g = y_i y_j^{-1}$, say) that (ii) is independent. In fact, by abelianizing this subgroup (i.e., by counting the exponents in a relator) we have relations $(6, -6) = 0$ from (i) and $(1, 1) = 0$ from (ii), in $\mathbb{Z}^2$, thus (i) is also independent.

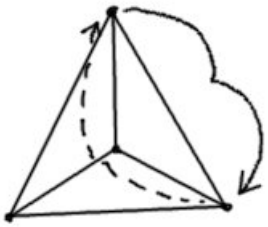

Figure 2.10: The motion of $y_3 y_2^{-1} y_3$ is effectively a rotation about the edge connecting the center vertex to the vertex in position 1.

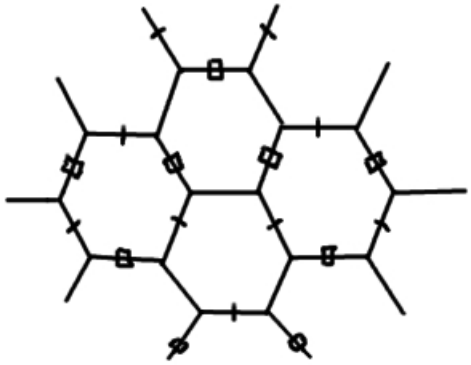

Figure 2.11: The Cayley graph for the quotient which would otherwise result in S_4 after disposing of relation set iii.

2.5 Action of $\pi_1(C(K_4))$ on F_3

Our space $C(K_4)$ is a specific case of the more general space of images of the $(n-2)$-skeleton of the n-simplex linearly embedded in $\mathbb{R}^n$. For the simplest such case, $n = 2$, we get the configuration spaces of 3 points $(\Delta^2)^0$ in the plane, both labeled and unlabeled, giving fundamental groups known classically as the *pure braid group on 3 strands* PB_3, and the *braid group on 3 strands* B_3, respectively. Both PB_n and B_n are realized as subgroups of $Aut(F_n)$ by considering the action of loops in the configuration space of n points in the plane on the fundamental

Figure 2.12: The motion of a generator y_i, acting trivially on a loop a_i in the complement of a configuration.

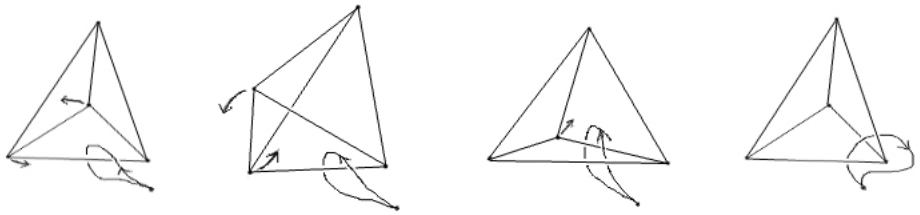

Figure 2.13: The generator y_1 sends a_2 to $a_1 a_2^{-1}$ (where concatenation of loops in F_3 is read from right to left).

group of the complement of a configuration (i.e., the n-punctured disc), which is F_n. The situation for $\pi_1(C(K_4))$ is similar, since the complement of a linearly embedded tetrahedral graph in $\mathbb{R}^3$ has fundamental group F_3, but here a rotation of the tetrahedron by 2π effects the trivial action on F_3. That is, this loop, τ, is in the kernel of the induced map $\psi : \pi_1(C(K_4)) \to Aut(F_3)$. By labeling the generators of F_3 in correspondence with the y_i's of $\pi_1(C(K_4))$, (see figure 2.12), we have that

$$\psi(y_i^2)(a) = a_i a a_i^{-1},$$

for $a \in F_3$ and a_i the generator of F_3 corresponding to y_i. Thus $\psi|_{\pi_1(Emb(K_4,\mathbb{R}^3))}$ is quotienting by the $\mathbb{Z}_2$ factor followed by the natural identification $F_3 \cong Inn(F_3)$.

The action of $\pi_1(C(K_4))$ on F_3 is given by the identities

$$y_i \cdot a_j = a_i a_j^{-1}$$

if $i \neq j$ and otherwise

$$y_i \cdot a_i = a_i,$$

as seen in figures 2.12, 2.13. The generators of $\pi_1(C(K_4))$ are thus sent to square roots of conjugation in $Aut(F_3)$.

CHAPTER 3

HIGHER DIMENSIONAL ANALOG

3.1 Codimension 2 Skeleton of a Simplex

This result can be generalized to a higher dimensional analog involving $Emb((\Delta^n)^{n-2}, \mathbb{R}^n)$, where $(\Delta^n)^{n-2}$ is the $(n-2)$-skeleton of the n-simplex, for $n > 3$. (The case $n = 2$ gives rise to an Eilenberg-Maclane space for the braid group on 3 strands. See [17], [11].) That we consider the $(n-2)$-skeleton insures that no n of the $n+1$ vertices lie in the same $(n-2)$-hyperplane, since the induced $(n-2)$-complex on these vertices is a simplicial $(n-2)$-sphere, which cannot topologically embed in $\mathbb{R}^{n-2}$. Then any n vertices span a codimension-1 hyperplane, and the $(n+1)$th vertex can occupy any point outside of the hyperplane or any point of $(n+1)$ open, simply connected disjoint regions in that hyperplane, as the next proposition makes explicit.

Proposition 3.1.1. *Let $(\Delta^n)^{n-2}$ be linnearly embedded in $\mathbb{R}^{n-1}$ (identify $(\Delta^n)^{n-2}$ with the image of its embedding). Then exactly one vertex c of $(\Delta^n)^0$ is in the interior of the convex hull of $(\Delta^n)^0$. Furthermore, let v be some extremal vertex, and $0 \leq i \leq n-2$ enumerate the vertices $v_i \in (\Delta^n)^0 \setminus \{c, v\}$ and let n_i be the outward normal vector to the $(n-2)$-face $(\Delta^n)^0 \setminus \{v, v_i\}$. Then for an embedding with c the interior point, v can occupy precisely any of the points in the open conical region*

$$c + \{w \in \mathbb{R}^{n-1} \mid \langle w, n_i \rangle > 0 \text{ for } 0 \leq \mathrm{i} \leq \mathrm{n} - 3\}.$$

(See figure 3.1.)

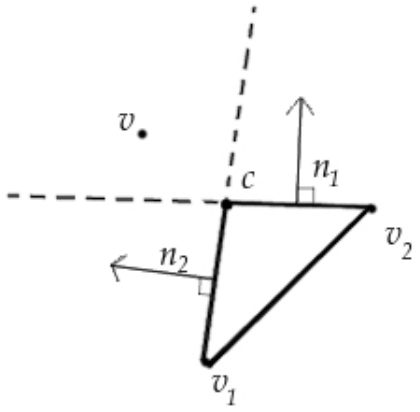

Figure 3.1: When $v \in c + \{w \in \mathbb{R}^2 | \langle w, n_i \rangle > 0; i = 1, 2\}$, c is in the interior of the triangle spanned by the v's.

Proof. That there is no more than one interior vertex is noted above: the complex induced on any n vertices is a copy of $(\Delta^{n-1})^{n-2}$, which is a topological sphere and doesn't embed in $\mathbb{R}^{n-2}$. Nor can the $(n+1)$th vertex lie on the boundary of the convex hull of the other vertices, since this boundary is in the image of the $(n-2)$-skeleton of the $(n-1)$-simplex. That there is one vertex interior to the convex hull of the others is a corollary to Radon's Theorem:

Theorem 3.1.2. *Given $n+1$ vertices V in $\mathbb{R}^{n-1}$, V can be partitioned into two disjoint non-empty sets such that the intersection of their respective convex hulls is non-empty (such a point is called a* Radon point*).*

For a proof see [24]. In our case, suppose both sets contain more than 1 vertex. Then the set with more vertices contains at most $n-1$ vertices and so each set is contained in an $(n-2)$-face which implies the $(n-2)$-skeleton of the n-simplex intersects itself away from the vertices. Then it must be the case that one set contains one vertex, and it is interior to the convex hull of the others. Finally, if

we fix a vertex c to be in the interior of the convex hull of the others, and allow a vertex v to vary, we must have that c is interior to the image of the convex hull of $(\Delta^n)^0$ under a rank 1 linear map to $\mathbb{R}$, so that for each i we have $\langle v - c, n_i \rangle > 0$ and so v is indeed in the open conical region defined above. (See figure 3.2.) $\square$

It is worth noting that such embeddings do exist. To see this note that the $(n-2)$-skeleton of Δ^n is the $(n-2)$-skeleton of the Δ^{n-1} we get by removing a vertex c, together with those $(n-2)$-faces of Δ^n that contain c. The former is a topological sphere, while the latter is the cone

$$\big((\Delta^{n-1})^{n-3} \times I\big)/\big((\Delta^{n-1})^{n-3} \times \{0\}\big)$$

thought of as a cone to the point c. When c is the origin of $\mathbb{R}^{n-1}$ and is inside the embedded $\partial\Delta^{n-1}$, this cone does not contain faces which intersect, since for $t \in (0,1]$ the embedded $(\Delta^{n-1})^{n-3} \times \{t\}$ is sitting in the embedded sphere $t(\Delta^{n-1})^{n-2}$, i.e., scaled from c by t,and these spheres are disjoint for distinct values $t_0 \neq t_1$.

Theorem 3.1.3. *The space $Emb((\Delta^n)^{n-2}, \mathbb{R}^n)$ of labeled linear embeddings of $(\Delta^n)^{n-2}$ into $\mathbb{R}^n$, for $n > 2$, is homotopy equivalent to $(\bigvee^n S^1) \times SO(n)$.*

Proof. The proof is directly analogous to Theorem 2.1.1. From Proposition , when the $(n+1)$th vertex is moved into the codimension-1 plane spanned by the others it must be in one of $n+1$ $(n-1)$-balls, which connect the upper half space to the lower half space. The space is thus a fiber product with fiber homotopy equivalent to a wedge of n circles. The base space is the space of embeddings of the labeled $(n-1)$-simplex in $\mathbb{R}^n$ which can be viewed as the space of ordered, positively

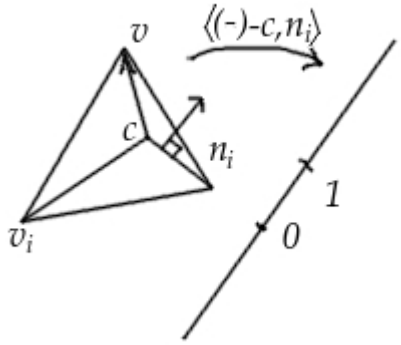

Figure 3.2: The mapping $v \mapsto \langle v - c, n_i \rangle$. Note that c is mapped into the interior of the image so that $\langle v - c, n_i \rangle > 0$, for each i.

oriented frames in the tangent bundle of $\mathbb{R}^n$, which has the homotopy type of $SO(n)$ by the Gram-Schmidt process. The bundle is again trivial by defining the analogous trivializing affine linear map to a typical fiber. The space is thus homotopically equivalent to $(\bigvee^n S^1) \times SO(n)$. □

3.2 An Analogue to Pyramids and Simplex Regularization

We next define a compact low dimensional model of $C((\Delta^n)^{n-2}, \mathbb{R}^n)$, analogously to that in section 2.3. Let $\mathcal{P}_n$ be those simplices in $\mathbb{R}^n$ with $A(n)$ symmetry (i.e., one face is regular, and the other vertex is equidistant to each vertex of that face), with barycenter at the origin, and such that the height is in $[0, \sqrt{\frac{n+1}{2n}}]$, and call these *pyramids*. We define a deformation retraction from $C((\Delta^n)^{n-2}, \mathbb{R}^n)$ to $\mathcal{P}_n$, first by regularizing the non-degenrate simplices. The idea is to increase the volume of the insphere while fixing the volume of the simplex. By symmetry such a flow is stationary on the regular simplices. We show that every trajectory results in a

regular simplex.

Lemma 3.2.1. *For r_x the inradius of an n-simplex x in $\mathbb{R}^n$ we have*

$$r_x = n \cdot \mathrm{Vol}(x)/\mathrm{Vol}(\partial x)$$

Proof. Realize x as a cone over ∂x to the incenter. Partition this cone into the cones over each face f_i. The volume of the cone over f_i is $\frac{1}{n} \cdot r_x \cdot \mathrm{Vol}(f_i)$. Summing over the faces gives the result. (See figure 3.3). □

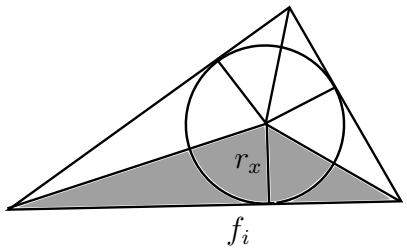

Figure 3.3: The volume of the simplex is disassembled into simplices with height r_x above base face f_i.

By the above, flowing along the gradient of Vol(insphere(x)) constrained to a fixed volume is the same as flowing to minimize the surface volume, with the same constraint. We consider the component of this flow in the direction which fixes a base face f_v and moves its opposite vertex v at height H above f_v, to minimize $\mathrm{Vol}(\partial x_t)$ to prove the following.

Lemma 3.2.2. *The flow which minimizes the surface volume of an n-simplex x in $\mathbb{R}^n$, subject to maintaining a fixed volume, results in a simplex where each vertex is directly over the incenter of its oppose face.*

Proof. Let the n $(n-2)$-dimensional faces of f_v be indexed as g_i, and denote the $(n-1)$-dimensional face containing g_i and v with $\bar{g}_i$. Let x_i be the signed

distance from the projection of v on the hyperplane containing f_v to g_i, signed so that x_i is positive whenever the projection of v is in f_v (see figure 3.4). We have $\mathrm{Vol}(\bar{g}_i) = \frac{1}{(n-1)} \cdot \mathrm{Vol}(g_i) \cdot \sqrt{H^2 + x_i^2}$ so that

$$\mathrm{Vol}(\partial x) = \mathrm{Vol}(f_v) + \frac{1}{(n-1)} \sum \mathrm{Vol}(g_i) \sqrt{H^2 + x_i^2}.$$

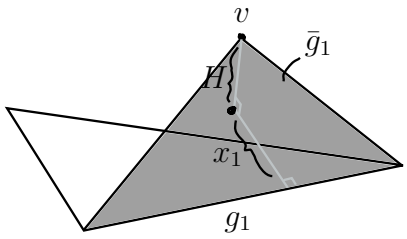

Figure 3.4: This figures illustrates x_i, g_i and $\bar{g}_i$ for the $n = 3$ case.

Any x_i depends affine-linearly on the others, since removing any one gives a coordinate system, so that

$$1 = \sum C_i x_i \tag{3.1}$$

for some constants C_i. The value of x_i for v over the ith vertex, for which all other x_j's are 0, is the altitude A_i of that vertex in f_v, giving $C_i = \frac{1}{A_i}$ and

$$A_i \mathrm{Vol}(g_i) = (n-1)\mathrm{Vol}(f_v). \tag{3.2}$$

Then (1) gives the constraint $\sum \frac{x_i}{A_i} = 1$ and using the method of Lagrange multipliers we get the system

$$\sum \frac{x_i}{A_i} = 1$$

and

$$\frac{1}{(n-1)} \frac{\mathrm{Vol}(g_i) \cdot x_i}{\sqrt{H^2 + x_i^2}} = \frac{\lambda}{A_i},$$

which using (2) simplifies to

$$\mathrm{Vol}(f_v) \cdot \frac{x_i}{\sqrt{H^2 + x_i^2}} = \lambda$$

which gives

$$v$$

implying

$$x_i^2(H^2 + x_j^2) = x_j^2(H^2 + x_i^2)$$

which necessitates $x_i = x_j$ since both are positive where a minimum is achieved. Therefore volume of boundary is minimized when the vertices are directly over the incenters of their respective opposite faces.

It remains to argue that such a trajectory actual terminates in a simplex with the property that the vertices are directly over the incenters of their opposite faces, as opposed to escaping to "infinity" or limiting to more than a single point.

Our flow is for simplices of fixed volume and will increase the volume bounded by the insphere. Note first that if we have vertices of arbitrary distance d from the incenter, then the cone formed by the vertex and the insphere (i.e., truncate it where its boundary intersects the insphere) is contained in the simplex x_t, and has volume with $\liminf$ equal to that of $d * c * (1/n)$ where c is the volume of the $(n-1)$-ball spanned by a great sphere of the insphere. Then, that the volume of x_t is fixed and is an upper bound for this cone necessitates that the inradius vanishes, contradicting the construction of the flow. Also note that if ℓ is the altitude of v and w is the closest vertex of x to v with edge length $|v - w|$, then for $2r$ the indiameter, we have $2r \leq \ell \leq |v-w|$, so that again r must vanish, contradicting the construction of the flow. (Figure 3.5 illustrates these two arguments). Translation to infinity is clearly not a concern. For example we can further stipulate that the incenter is fixed at the origin.

Finally, getting arbitrarily close to the critical set gives that each vertex gets arbitrarily close to being directly over the incenter of the opposite face, so that the flow results in a single limiting simplex.

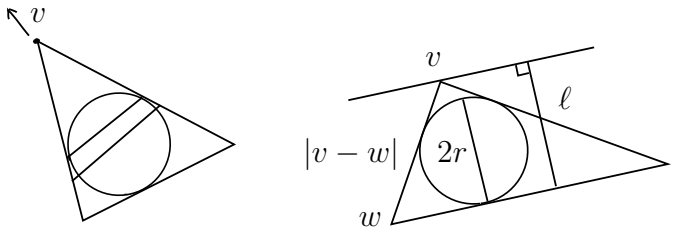

Figure 3.5: The trajectory does not escape to infinity.

□

Lemma 3.2.3. *A simplex for which each vertex orthogonally projects to the incenter of the opposite face is a regular simplex.*

Proof. Let v, w be vertices of the simplex x, c_v be the incenter of the face f_v opposite v and r_w be the outward pointing radial vector from c_v to the codimension 2 face excluding w and v (Figure 3.6 is helpful). Note that the r_w form congruent right triangles with $v - c_v$, and that on the ith face the gradient of the distance to f_v, (at $c_v + r_w$ in f_w) is the hypotenuse of the right triangle containing r_w. Thus the point on $v - c_v$ which is equidistant to some face and to c_v is actually the incenter c_x.

It is therefore the case that c_x projects orthogonally to c_v and all other faces have equal pitch relative to f_v. That is, for c_w the outward pointing vector from c_x to f_w realizing the inradius, we have that $c_w \cdot c_u = c_w \cdot c_y$ for all distinct u, w, y. It follows that the simplex they define has full symmetry. □

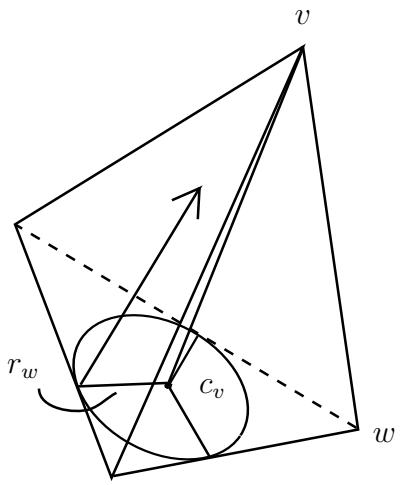

Figure 3.6: The condition that each vertex is over its opposite incenter implies regularity.

The previous two lemmas piece together to give the following theorem.

Theorem 3.2.4. *The space of linearly embedded n-simplices in $\mathbb{R}^n$ deformation retracts to that of the regular ones. In particular, this is achieved by the flow which increases the inradius while fixing the entire volume.*

3.3 Gluing Deformation Retractions Together

For those close to being degenerate, we will make use of a greatest solid angle function α. We require the following lemma.

Lemma 3.3.1. *Let V_{n-1} be the $(n-1)$-volume of the unit $(n-1)$-sphere, for $n > 2$. The sum S of the solid angles of (the $(n-2)$-skeleton of) an n-simplex in $\mathbb{R}^n$ is sharply bounded by $(0, V_{n-1}/2]$.*

Proof. Consider first only non-degenerate simplices. The idea is to translate, for each of $n+1$ vertices, a copy of the n-simplex, to have its ith vertex at 0. The $n+1$ cones C_i which are formed by extending each of these outward, along with their reflections $-C_i$ through 0, give $2n+2$ regions whose interiors are pairwise disjoint. Intersection with a unit sphere S^{n-1} then gives that

$$V_{n-1} \geq \sum_i \text{Vol}(C_i \cap S^{n-1}) + \sum_i \text{Vol}(-C_i \cap S^{n-1}) = 2S.$$

Specifically, put the 0th vertex at the origin and let x_i be the ith vertex, for $1 \leq i \leq n$ ranging over the other n vertices. Then

$$C_0 = \textit{convex span}\{x_i\} = \sum a_i x_i$$

for $a_i \geq 0$, and

$$\begin{aligned} C_i &= \textit{convex span}(\{x_j - x_i\}_{j \neq i} \cup \{-x_i\}) \\ &= (\sum_j a_j(x_j - x_i)) - a_i x_i. \end{aligned}$$

Putting these into coordinates x_i gives C_i as

$$(a_1, a_2, \ldots, a_{i-1}, -\sum_j a_j, a_{i+1}, \ldots, a_n),$$

from which it is clear that for any $i \neq j$ we have

$$\textit{int}(C_i) \cap \textit{int}(C_j) = \textit{int}(C_i) \cap \textit{int}(-C_j) = \varnothing.$$

It remains to show the bounds are sharp. The sum being 0 could only happen for a degenerate simplex, but Proposition 3.1 says that for such a simplex one vertex is interior to the convex hull of the other n points, so the solid angle here is a hemisphere, proving the bounds are sharp. □

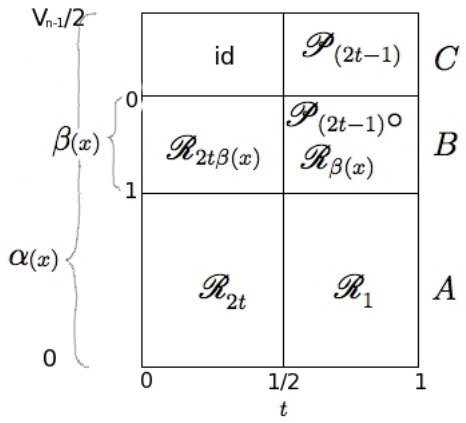

Figure 3.7: The schematic for gluing together the regularization deformation retraction and the preferred point deformation retraction.

The procedure to handle the degenerate cases in the general dimension n case will differ from the 3 dimensional case, because in general we use a non-linear deformation retraction to regularize the simplices, as opposed to the linear method in dimension 3. Consequently, the limiting path of the vertex with successively larger solid angles is not defined without considerable further work. Instead, we will glue the regularization deformation retraction to a second deformation retraction which is defined only in a neighborhood of the degenerate simplices.

As above, let V_{n-1} be the volume of the unit $(n-1)$-sphere. Define some cut off point $\ell \in (V_{n-1}/4, V_{n-1}/2)$ and let $\beta(x)$ be the affine linear reparametrization of $\alpha(x)$ which has $\beta(\alpha^{-1}(V_{n-1}/4)) = 1$ and $\beta(\alpha^{-1}(\ell)) = 0$. Let $B = \beta^{-1}[0,1]$, $A = \beta^{-1}[1,\infty)$, $C = \beta^{-1}(-\infty, 0]$, form a closed cover of $C((\Delta^n)^{n-2}, \mathbb{R}^n)$ (follow along with figure 3.7). We define a deformation retraction $\mathscr{P}_t$ on $B \cup C$ to $\mathcal{P}_n$, called the *preferred point deformation retraction*, which moves the vertex of large solid angle v in the hyperplane parallel to W_x, the face opposite v, in a constant

velocity path towards the point in this hyperplane directly over the barycenter c_x of W_x, followed by regularizing W_x in its own hyperplane using the geometric flow introduced earlier in this section, and extended to be an isometry in the orthogonal complement. Finally a normalization of edge lengths, and a translation, has $\mathscr{P}_t$ arrive in $\mathcal{P}_n$. Next we glue.

Let $\mathscr{R}_t$ be the volume-fixing insphere-maximizing flow defined above, followed by normalization of edge lengths to arrive in $\mathcal{P}_n$, and define $\mathscr{P}_{(2t-1)} \circ \mathscr{R}_{\beta(x)}$ to be $\mathscr{R}_{\beta(x)}$ followed by the preferred point deformation retraction of x by the parameter $2t-1$ (i.e., if $\mathscr{R}_{\beta(x)}(x)$ reduces the greatest solid angle to less than $V_{n-1}/4$ then strictly speaking $\mathscr{P}_{(2t-1)}$ is not defined here). The maps agree on the lines separating regions of the schematic in figure 3.7, so the deformation retraction glues. The picture is this: flow along $\mathscr{R}$ toward regularization. The parameter β, where it is used, is used to proportionally go less of the entire way toward the regular simplices. At the point $\mathscr{R}_{\beta(x)}$ we let the preferred point flow take over. As β decreases to 0 there is proportionately less regularization that has been done, until $\beta = 0$ and the only the prefered point flow is used.

The Theorem of Van Kampen applies to $\mathcal{P}_n$. The half-high pyramids have as fundamental group the subgroup of Spin(n) (the double cover of $SO(n)$) which double covers the copy of $A_{n-1} < SO(n-1) < SO(n)$, the alternating group, which comes from orientation preserving symmetries of the symmetrical face. The regular pyramids have as fundamental group the subgroup of Spin(n) which double covers the copy of $A_n < SO(n)$, and the degenerate pyramids have as fundamental group the subgroup of Spin(n) which double covers the copy of $S_{n-1} < SO(n)$, the

symmetric group which permutes the extremal vertices. Hence

Theorem 3.3.2. *The space of $(n-2)$-skeleta of n-simplices in $\mathbb{R}^n$ is homotopy equivalent to the double mapping cylinder*

$$SO(n)/A_n \leftarrow SO(n)/A_{n-1} \rightarrow SO(n)/S_{n-1}$$

where the maps are the obvious ones given by the decomposition of pyramids into those half-high, those which are regular and those which are degenerate.

Proof. The symmetries of the spaces are straightforward, as are the inclusions. The proof follows from Van Kampen's Theorem. □

Finally, let us observe by analogy to section 5 that the fundamental group of the complement of a configuration of $(\Delta^n)^{n-2}$ in $\mathbb{R}^n$ is F_n, the free group on n generators, as can be seen from looking at a degenerate configuration, which separates a hyperplane $\mathbb{R}^{n-1} \cong P \subset \mathbb{R}^n$ into n $(n-1)$-balls and one thickened $(n-2)$-sphere. A loop in this space, based in the $(n-2)$-sphere, say, is generated by paths which pass into the northern half-space in $\mathbb{R}^n$, pass through one of the $(n-1)$-balls, and return via the southern half-space. Thus the configuration space $C((\Delta^n)^{n-2}, \mathbb{R}^n)$ gives rise to an action of $2A_n *_{2A_{n-1}} 2S_{n-1}$ on F_n. We omit further details.

CHAPTER 4

THE CASE OF $C((\Delta^{N+1})^{N-2}, \mathbb{R}^N)$

4.1 Increasing the Number of Vertices

In this section we increase the number of vertices by increasing the dimension of the simplex, while keeping both the skeleton's dimension and the ambient dimension the same. We seek to compare the homotopy type of $C((\Delta^{n+1})^{n-2}, \mathbb{R}^n)$ with that of $C((\Delta^n)^{n-2}, \mathbb{R}^n)$, using the methods developed in chapter 3.

Lemma 4.1.1. *For $n > 2$ the codimension 3 skeleton of Δ^{n+1} embedded in $\mathbb{R}^n$, has either one vertex interior to the convex hull of the others, or has exactly one edge which intersects the $n-1$ face spanning the other n vertices.*

Proof. Let $x \in C((\Delta^{n+1})^{n-2}, \mathbb{R}^n)$. We may apply Radon's Theorem. Let p be a Radon point (see Theorem 3.1.2) in the intersection of two faces F_1, F_2. Then one of these two faces is of dimension at least $n-1$, since otherwise the $(n-2)$-skeleton is not embedded, so that the other face is at most of dimension 1. In the case that the lower dimensional face, say F_1, is dimension one, then $(F_2)^{n-2}$ is a simplicial sphere in the dimension $n-1$ hyperplane H it spans. It is possible that one vertex v_1 of F_1 is in H. To show that the other vertex v_2 in F_1 cannot be in H, we generalize the argument that K_5 is non-planar (see figure 4.1) Let W be the vertices of F_2 union $\{v_1\}$. By remarks in section 7, here we have that some vertex $w \in W$ is in the interior (in H) of the convex hull of the other vertices in W. Then for $w \neq u \in W$, u is exterior to the $(n-2)$-sphere formed by the $(n-2)$-skeleton of $W \setminus \{u\}$. Suppose that v_2 is also in H. It is connected by edges to each such u, so

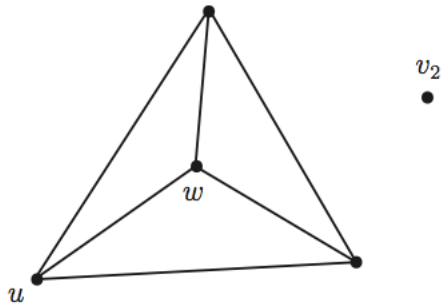

Figure 4.1: The graph K_5 is non-planar since a fifth vertex put in one of the four regions above is necessarily separated from one of the four vertices. Similarly $(\Delta^{n+1})^{n-2}$ does not embed in $\mathbb{R}^{n-1}$ for $n \geq 2$.

cannot be contained in any of the spheres thus formed, so it must be exterior to F_2, but then cannot connect to w without intersecting F_2. This shows that when the lower dimensional face is dimension one the Radon point is unique. In the case the lower dimensional face is dimension 0 this is immediate. The Radon point p thus distinguishes either two vertices whose edge contains p, or one interior vertex.

On the other hand, given any non-degenerate configuration of the $(n-2)$-skeleton of an n-simplex in $\mathbb{R}^n$, with some marked vertex v, we can introduce an $(n+2)$th vertex w and the induced $(n-2)$-faces, by placing w anywhere in the interior of the inward pointing cone at v, formed by its edges. To show that the $(n-2)$-skeleton doesn't intersect itself, let the first n vertices be the standard basis e_i of $\mathbb{R}^n$, the $(n+1)$th vertex be the origin, and the $(n+2)$th vertex be in the interior of the first orthant (see figure 4.2). This is sufficiently general, since any non-degenerate n-simplex in $\mathbb{R}^n$ is sent here by an invertible affine linear map, but we will further put the $(n+2)$th vertex at $(k, \ldots, k)$, for some $k > 0$, for simplicity,

since self-intersection will only change when we change the strict inequalities which partition the vertices into interiors of half-spaces formed by the others. Thus, we need only check the specific case $k = \frac{1}{n}$ and the cases to either side. Let a be in the convex span of some $n-1$ vertices amongst $\{e_i\} \cup \{0\} \cup \{(1, \ldots, 1)\}$. We have

$$a = (a_1, \ldots, a_n) + a_{n+2}(k, \ldots, k)$$

where $a_i = 0$ for at least 3 values of i (possibly including the coefficient a_{n+1} of the vertex at the origin). Let b be the same point but with coefficients coming from another face, i.e.,

$$b = (b_1, \ldots, b_n) + b_{n+2}(k, \ldots, k) = a.$$

Then for $a_i = 0$, $i \leq n$, we have that this coordinate of a which is $a_{n+2}k$ is less than or equal to the other coordinates, so that the same holds for b and thus $b_i = 0$. That values $1 \leq i \leq n$ for which $a_i = 0$ are the same as those for which $b_i = 0$ contradicts that the $(n-2)$-faces are different. Therefore, the faces do not intersect. □

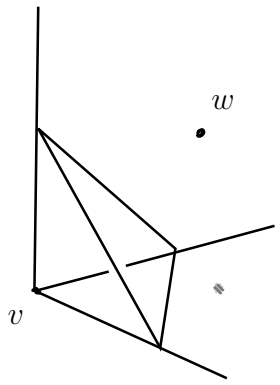

Figure 4.2: The $(n+2)$th vertex w is in the cone formed by the edges emanating from v, which is in this case the first orthant.

The above lemma say that the picture for general n is much as it is for $n = 3$:

there is either an edge intersecting the interior of an $(n-1)$-cell (which is not a part of our skeleton) or there is a vertex interior to the convex hull of the others (see figure 4.3).

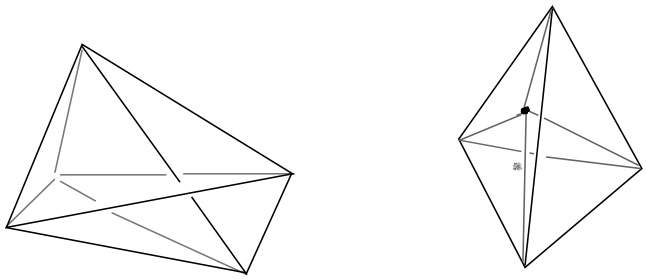

Figure 4.3: Generically, either some vertex is interior to the convex hull of the others or some specific edge intersects its opposite face.

4.2 Another Pyramid-like Space

A space analogous to pyramids exists for $C((\Delta^{n+1})^{n-2}, \mathbb{R}^n)$. Let this space consist of those configurations such that $n+1$ of the vertices form a regular, unit edge length image S of $(\Delta^n)^{n-2}$, and where the $(n+2)$th vertex is on a line connecting the centroid of one face F of S to the centroid of S, at a height between the centroid and $\sqrt{\frac{n+1}{2n}}$ above F. (The height of a regular unit edge length n-simplex is $\sqrt{\frac{n+1}{2n}}$.) Denote this space with $\mathcal{Q}_n$.

Let $\mathcal{I} \subset \mathcal{Q}_n$ be those with Radon point a vertex interior to the convex hull of the others, let $\mathcal{E}$ be those with Radon point in the interior of an edge, and $\mathcal{B}$ be the others, i.e., those with Radon point a vertex in the boundary of the convex hull of the others (see figure 4.4). We will use a deformation retraction

of $C(\Delta^n, \mathbb{R}^n)$ to the space of regular simplices to define a deformation retraction from $C((\Delta^{n+1})^{n-2}, \mathbb{R}^n)$ to $\mathcal{Q}_n$. For the subspace $\mathcal{E}$, we will apply slightly different deformation retractions to both halves of its elements by gluing along their shared face. For this we require a linear deformation retraction following what was done in Section 3.

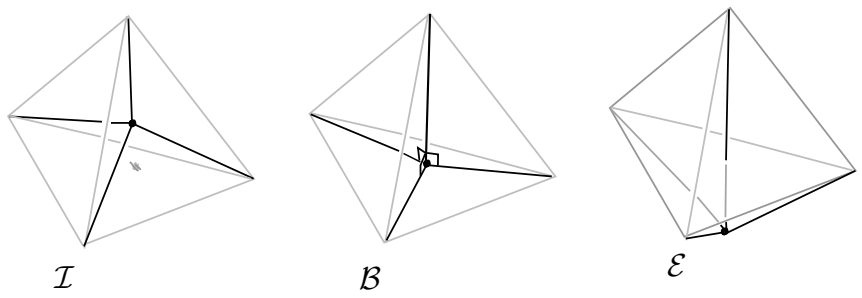

Figure 4.4: The three types of configurations in $\mathcal{Q}_n$

4.3 A Linear Regularization

Theorem 4.3.1. *The deformation retraction of Theorem 3.2.4 is achieved with a linear flow.*

Proof. Let A be the $n \times n$ symmetric matrix whose columns form a unit edge length simplex. Explicitly A has μ for each entry on its diagonal and ν for each entry off the diagonal where $\mu^2 + (n-1)\nu^2 = 1$ and $2(\mu - \nu)^2 = 1$, so that

$$\mu = \frac{n + \sqrt{n+1} - 1}{\sqrt{2}n} \qquad \text{and} \qquad \nu = \frac{\sqrt{n+1} - 1}{\sqrt{2}n}.$$

Let B_i be the $n \times n$ identity matrix I with the ith row replaced by $[-1, \ldots, -1]$. The matrix B_i acts on the right as a column operator to change bases between

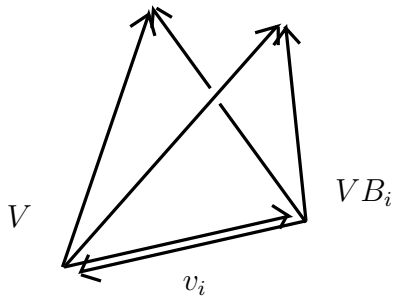

Figure 4.5: B_i swaps V for the basis at v_i which spans the same simplex as V.

vertices of an n-simplex. I.e., given a matrix V whose columns form a basis, the columns of VB_i are those eminating from Ve_i to 0 and to each of the other Ve_j's (see figure 4.5). Let $B \in \{B_i\}$. Note that

$$AB = QA$$

for some $Q \in O(n)$ (this is obvious, geometrically). We have $B^2 = I$ and $Q^{-1} = ABA^{-1}$ so $Q^{-1} = Q^T = Q$ and

$$B^T = (A^{-1}QA)^T = AQ^{-1}A^{-1} = A^2BA^{-2}.$$

Let

$$\Omega_t(x) = \Big[(1-t)xA^{-1} + txA^{-1}((xA^{-1})^T(xA^{-1}))^{-1/2}\Big]A.$$

Then $\Omega_t(x) \cdot A^{-1}$ is the Löwdin deformation retraction of xA^{-1} to $O(n)$, and so $\Omega_t(x)$ gives a linear path from x to $O(n) \cdot A$ (see figure 4.6). We compute $\Omega_t(xB)$ to show equivariance: $\Omega_t(xB) = \Omega_t(x)B$.

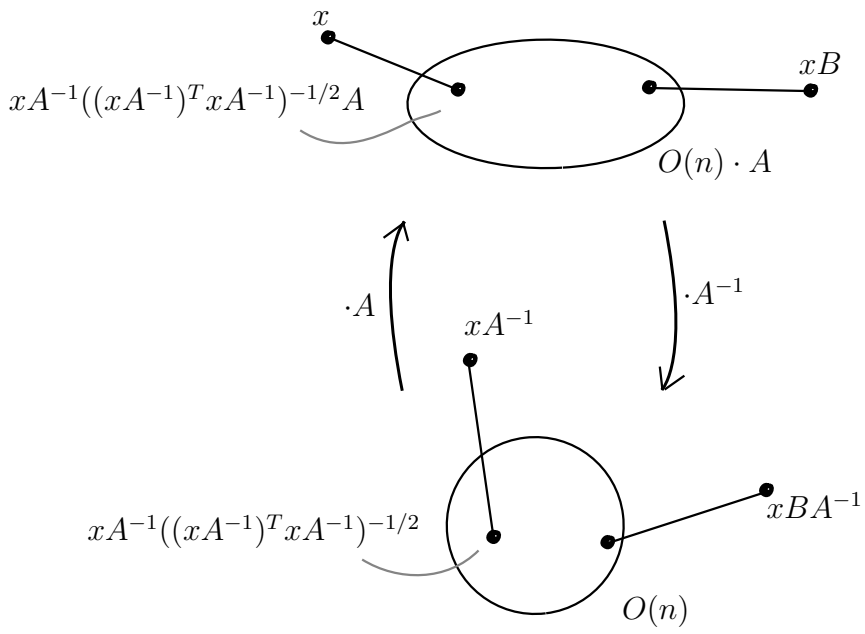

Figure 4.6: The S_n equivariant orthogonalization is conjugated to give a S_{n+1} equivariant regularization. The line segments are the deformation retractions in $GL(n)$.

$$\begin{aligned}
\Omega_t(xB) &= \Big[(1-t)xBA^{-1} + txBA^{-1}((xBA^{-1})^T(xBA^{-1}))^{-1/2}\Big]A \\
&= \Big[(1-t)xA^{-1}Q + txA^{-1}Q((xA^{-1}Q)^T xA^{-1}Q)^{-1/2}\Big]A \\
&= \Big[(1-t)xA^{-1} + txA^{-1}((xA^{-1})^T(xA^{-1}))^{-1/2}\Big]QA \\
&= \Big[(1-t)xA^{-1} + txA^{-1}((xA^{-1})^T(xA^{-1}))^{-1/2}\Big]AB \\
&= \Omega_t(x)B,
\end{aligned}$$

so Ω_t is equivariant under B. The set $\{B_i\}$ generates a copy Γ of S_{n+1} (B_i acting on the vertices, in cycle notation, is the transposition $(0,i)$) so up to translation and scaling (see figure 4.7), $(O(n)\cdot A)/\Gamma$ is the space of regular simplices and Ω_t descends to the quotient $(GL(n)\cdot A)/\Gamma$, to give a linear (i.e., vertices move along linear paths) S_{n+1}-equivariant regularization of simplices in $\mathbb{R}^n$. $\square$

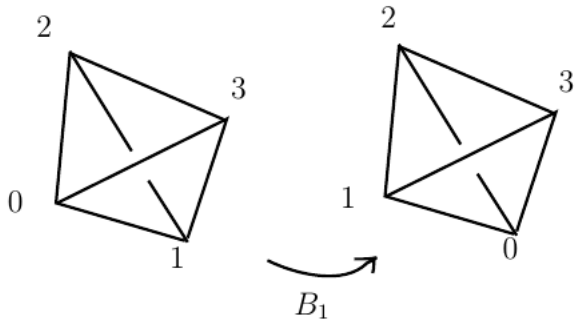

Figure 4.7: B_i is effectively the transposition $(0, i)$.

4.4 The Deformation Retraction

Theorem 4.4.1. *The space $C((\Delta^{n+1})^{n-2}, \mathbb{R}^n)$ deformation retracts to $\mathcal{Q}_n$, the pyramid model.*

Proof. We achieve the deformation retract in three steps, the first two of which are divided into 3 cases each.

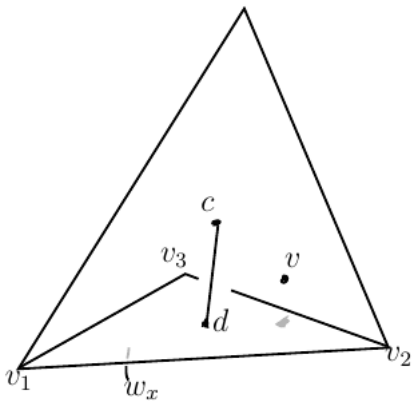

Figure 4.8: Realize v as a convex combination of c and the closest vertices v_i to v.

Step 1a. Let $x \in \mathcal{I}$ with interior vertex v. Let $\{v_i\}$, $1 \leq i \leq n$, be n of the closest vertices of x to v, and let c be the centroid of x, and d to be the centroid of the face W_x spanned by $\{v_i\}$ (see figure 4.8). We will move v to lie along the line segment connecting c to d. This can be done explicitly by putting v in barycentric coordinates

$$v = qc + \sum a_i v_i. \qquad \text{(with } q + \sum a_i = 1, \text{ and } q, a_i \geq 0\text{)}$$

Set $m = \min\{a_i\}$. Note that $m = q = 0$ cannot happen since this would put v in the $(n-2)$-skeleton of x (see figure 4.9). We have $3m \leq 1 - q$ and require a parameter $s(m, q)$ so as to send v to $(1-s)d + sc$ which is continuous on $0 \leq 3m \leq 1 - q \leq 0$ minus the origin, and for which $s(0, q) = 1$, $s(m, 0) = 0$ and $s(\frac{1}{3}(1-q), q) = q$ (so that if v is equidistant to two extremal vertices it gets sent to c, if it is in W_x it gets sent to d, and if it is on the line connecting c to d it is fixed). This is accomplished with

$$s(m, q) = (1 - q)\Big(1 - \frac{3m}{1-q}\Big)^{1/q} + q,$$

which we extend continuously by $s \equiv 0$ on $q = 0$ (see figure 4.10). Sending v to $(1-s)d + sc$ along the straight line path $v_t = (1-t)v + t(1-s)d + sc$ gives a retraction of $\mathcal{I}$ to the subspace of $\mathcal{I}$ with internal vertex along a radial segment connecting the barycenter to the center of a face.

Step 1b. Let $x \in \mathcal{E}$. We want to parallel transport the edge e containing the Radon point p so that the intersection of this edge with its opposite face W_x is at the barycenter d of that face. When one vertex v_1 of e is close to W_x we need the other vertex v_2 to move only a small distance so that step 1b can be continuously glued to step 1a. To do this, we follow the parallel transport with a sheer back in the direction that v_2 has moved, in the plane containing d and e, with origin at d,

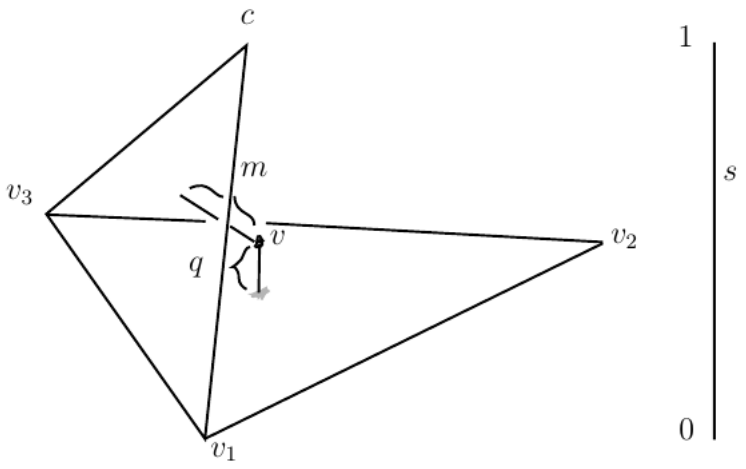

Figure 4.9: Using the parameters q, which is distance from the extremal face, and m, minimum distance to a face containing c, to define s.

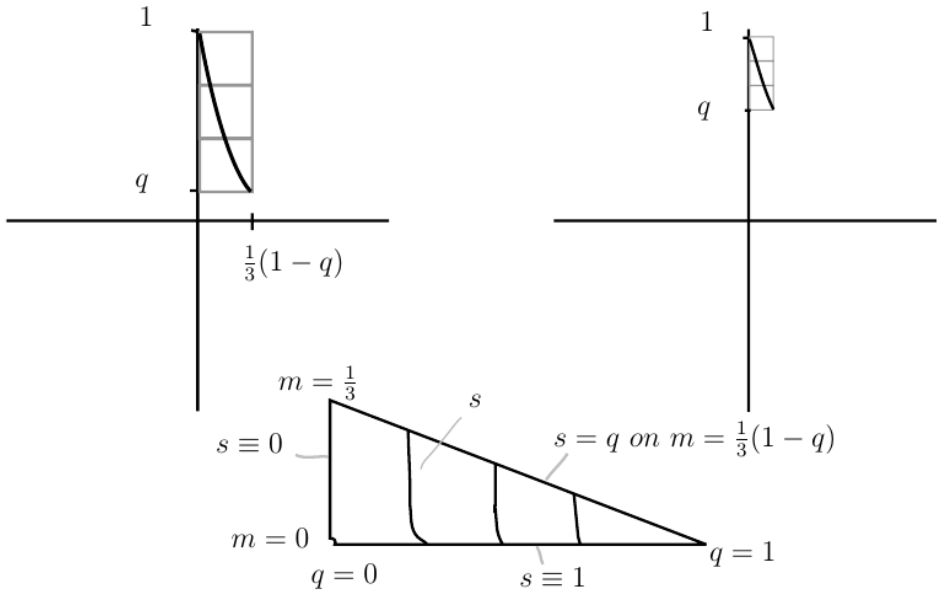

Figure 4.10: Graphs of s for smaller q (left), for larger q (right), and in the $q - m$ plane (bottom). Note the origin is excluded.

in proportion to $1 - \frac{v_1 - p}{v_2 - p}$. Explicitly, put $\ell_i = |v_i - p|$ (see figure 4.11), and send v_2 to $v_2 + \frac{\ell_1}{\ell_2}(d - p)$, send p to d, and send v_1 to $v_1 + \frac{(\ell_2 - \ell_1)\ell_1}{\ell_2^2}(d - p)$. Thus as we approach $\mathcal{B}$, ℓ_1/ℓ_2 approaches 0 and V_2 moves less and less.

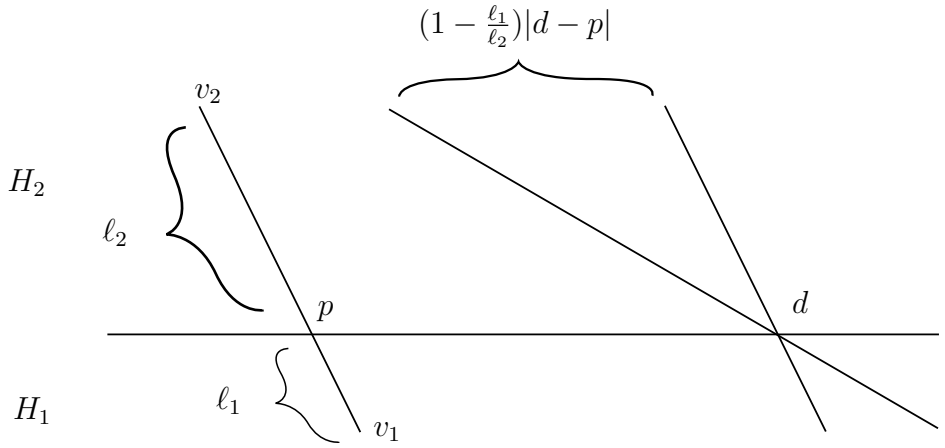

Figure 4.11: Parallel transport followed by a shear, with v_2 going back in the direction parallel transported.

Step 1c. These two deformation retractions agree on their respective extensions to $\mathcal{B}$. In both cases the extension is to send the Radon point vertex to the centroid of the $(n-1)$-face it is in, in a straight line path while fixing everything else.

At the end of step 1 the Radon point of each $x \in C((\Delta^{n+1})^{n-2}, \mathbb{R}^n)$ is along a ray extending from the centroid of x to the centroid of a face. For $0 \leq t \leq \frac{1}{3}$, let Λ_t be all three parts of step 1, simultaneously performed in the variable $3t$.

Step 2a. For $x \in \Lambda_{1/3}(\mathcal{I})$, using the same barycentric coordinates and function s as in 1a. we damp by the parameter $1 - s$ the regularization of the extremal n-simplex via Ω. Specifically, let $\omega : I \to \mathrm{Aff}(\mathbb{R}^n)$ be defined as the induced map from Ω as was done in section 3 (i.e., $\omega_x(t)$ is the transformation which takes W_x to $\Omega_t(W_x)$ and which takes $W_x^\perp$ to $(\Omega_t(W_x))^\perp$, preserving distance and orientation.)

For $x \in \Lambda_{1/3}(\mathcal{I})$ with $s \in (0,1)$, let

$$\Lambda_t(x) = \big(\omega_x\big((1-s(x))(3t-1)\big)\big)^{-1} \circ \Omega_{3t-1}.$$

Then Λ_{3t-1} extends to where $s \in \{0,1\}$ continuously (i.e., $\Lambda|_{s^{-1}(0)}$ keeps W_x fixed, $\Lambda|_{s^{-1}(1)} = \Omega_t|_{s^{-1}(1)}$).

Step 2b. For $x \in \Lambda_{1/3}(\mathcal{E})$ let ℓ_1, ℓ_2 be as in 1b. We will keep the shared face fixed and apply Ω to the half-space H_2 containing v_2. To the other half-space we deformation retract not to $\Omega_1(x)$ but to $L \cdot \Omega_1(x)$ where L scales in the direction of $W_x^{\perp}$ by $\frac{\ell_1}{\ell_2}$. Specifically, we have

$$x \mapsto (\omega_x(t))^{-1} \cdot \Omega_t(x)$$

on H_2 and

$$x \mapsto (\omega_x(t))^{-1} \cdot \bar{\Omega}_t(x)$$

on H_1, where $\bar{\Omega}_t(x) = (1-t)x + L\Omega_t(x)$.

Step 2c. For $x \in \Lambda_{1/3}(\mathcal{B})$ the the non-degenerate half of x is regularized by the process of 2a. This agrees with the limit of the process in 2b. as x approaches$\mathcal{B}$ from $\mathcal{E}$.

For $\frac{1}{3} \leq t \leq \frac{2}{3}$, let Λ_t be all three parts of step 2, simultaneously performed in the variable $3t-1$.

At the end of step 2 all that remains is to regularize W_x in the hyperplane it spans, and extend to an isometry on $W_x^{\perp}$. This is achieved by Theorem 4.3.1. This gives the final third of Λ. □

Theorem 4.4.2. *$C((\Delta^{n+1})^{n-2}, \mathbb{R}^n)$ is homotopy equivalent to $C((\Delta^n)^{n-2}, \mathbb{R}^n)$, moreover $\mathcal{Q}_n$ is homeomorphic to $\mathcal{P}_n$.*

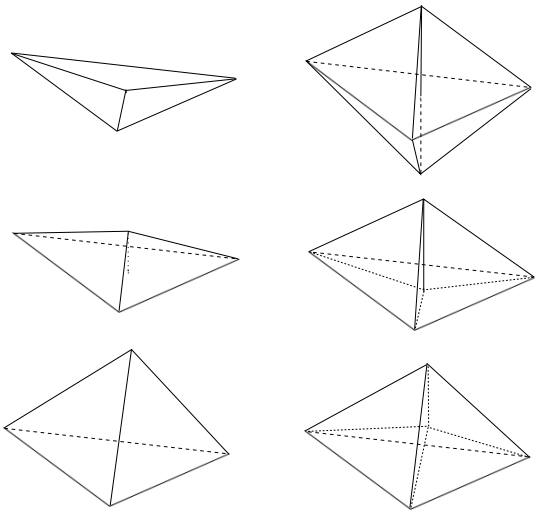

Figure 4.12: A comparison of the symmetries found in the K_4 and K_5 pyramidal cases. Note the equality of the symmetries between horizontally adjacent figures.

Proof. The deformation retraction above gives $C((\Delta^{n+1})^{n-2}, \mathbb{R}^n) \simeq \mathcal{Q}_n$. Both $\mathcal{Q}_n$ and $\mathcal{P}_n$ have subsets representing objects with the symmetry of an n-simplex in $\mathbb{R}^n$, and subsets representing objects with the symmetry of an $(n-1)$-simplex in $\mathbb{R}^n$. An obvious homeomorphism between $\mathcal{Q}_n$ and $\mathcal{P}_n$ is given by linearly corresponding the parameters which range between these respective subsets. (See figure 4.12) $\square$

CHAPTER 5

SMOOTH CONFIGURATIONS

5.1 Trivalent Polyhedral Graphs

In what follows a *graph* will be a simple, undirected graph. *Trivalent* means each vertex is incident to 3 edges. *3-connected* will mean that the removal of any pair of vertices and all their incident edges leaves a connected graph. A *polyhedral* graph is a 3-connected planar graph (note that because we are considering only trivalent graphs, we needn't specify whether complete graphs K_i for $i = 0, 1, 2, 3$ are polyhedral). A singleton set will be denoted 1. X^1 will denote a polyhedral graph.

In this chapter we calculate the homotopy type of the planar embedding component of any given trivalent polyhedral graph in $\mathbb{R}^3$. That this is a single component follows from a lemma below (see Corollary 5.1.1). We will denote this component by Emb_0, which will be in the C^∞ category, unless otherwise specified. For ease of computation we require C^∞ embeddings of graphs to be trivial near vertices (meaning there is a neighborhood U of each embedded vertex so that $(G \cap U, U)$ is diffeomorphic to a union of straight lines in some neighborhood of the origin of $\mathbb{R}^n$ (n=2 or 3)). (For an example of a non-trivial embedding, consider the curve $t\mathbf{v} + \mathbf{e}^{-\mathbf{1/t^2}} \sin(\mathbf{1/t})\mathbf{w} + \mathbf{e}^{-\mathbf{1/t^2}} \cos(\mathbf{1/t})\mathbf{x}$, for $\mathbf{v}, \mathbf{w}, \mathbf{x}$ an orthonormal basis. A second copy, off-set in phase, will wind around this curve an infinite number of times in any neighborhood of the origin, yet both are smooth). This implies that parallel tangents at a vertex come from opposite directions so there are no cusps. We require the same of 2-complexes (definition below), that when 2 embedded 2-cells

share the same tangent space they form a plane locally and not a flat crease.

Let $Emb_0(X^1 \coprod 1, S^3)$ be the those components of the embedding space of X^1 along with a disjoint point into S^3 which contain the planar embeddings. The space $Emb_0(X^1 \coprod 1, S^3)$ fibers over both restrictions giving the following two short exact sequences (the diagonals).

$$\begin{array}{ccccc} Emb_0(X^1, \mathbb{R}^3) & & & & \bigvee^n S^1 \\ & \overset{\tau}{\rightleftarrows} & & \nwarrow & \\ & & Emb_0(X^1 \coprod 1, S^3) & & \\ & \swarrow & & \searrow & \\ Emb_0(X^1, S^3) & & & & S^3 \end{array} \tag{5.1}$$

Here the lower maps are restrictions to respective components X^1 and 1. The fiber to the right is a handlebody, denoted by a wedge of n circles, where n is the 1st Betti number of X^1. The left fiber is the space we seek to understand. The arrow τ is a splitting, given by rotating S^3 by $f(1)^{-1}$ for each embedding f, and projecting along a predetermined stereographic projection from $1 \in S^3$.

By *2-complex* we mean a slight generalization of 2-dimensional Δ-complex, made up of abstract 2-cells (polygons), 1-cells (graph edges) and 0-cells (graph vertices), and the usual boundary maps (see [11]). The precise loosening of the definition from simplicial complex is that (1) the 2-cells are arbitrary polygons and (2) the boundary can be a union of lower dimensional cells.

Theorem 5.1.1. *For X^1 a trivalent polyhedral graph which is the 1-skeleton of the 2-complex X, $Emb_0(X^1, S^3) \simeq Emb(X, S^3)$, where Emb is the space of smooth planar embeddings in the C^∞ topology.*

Proof. We shall breakdown the theorem into lemmata. By *convex polyhedron* we mean the 2-complex associated to the boundary of a geometric convex polyhedron (i.e., a compact intersection of a finite number of closed half-spaces in $\mathbb{R}^3$), and not the geometric realization itself.

Lemma 5.1.2. *A polyhedral graph is the 1-skeleton of a unique convex polyhedron.*

Proof. Given a planar 2-connected graph X^1 and an embedding $f : X^1 \to \mathbb{R}^2$ we may define a 2-complex X such that the 1-skeleton of X is X^1, by compactifying the plane at infinity and using the subsequent 2-cell structure of S^2. Now suppose C is a cycle which is the boundary of a 2-cell under this assignment using f, (we will call such a cycle a *boundary cycle*) and without loss of generality, assume C is the extremal cycle, separating $f(X^1)$ from infinity, and suppose we have a second planar embedding g of X^1 under which C is neither innermost nor extremal (i.e., for both components K_i of $\mathbb{R}^2 \setminus C$, $K_i \cap X^1 \neq \varnothing$.) Let E be an edge of C and let F_i $i = 1, 2$ be the faces on either side of E under the mapping g. By supposition, neither F_i is C. Let A_i be the arc induced on the vertices of ∂F_i minus the end points of E (A_i is just a vertex when ∂F_i is a triangle). Note that A_1 is not connected to A_2 by a path which avoids C, since C separates the plane in the image of g. Note also that in the image of f, E is extremal and contained in both ∂F_i, so that one of A_i must not be connected to vertices in $int(C \setminus E)$ through a path which avoids ∂F_j (for $j \neq i$). □

Corollary 5.1.1. *For X^1 a polyhedral graph, the path component $Emb_0(X^1, \mathbb{R}^3)$ containing some planar embedding contains all planar embeddings.*

Proof. For two embeddings of X^1 in $\mathbb{R}^3 \subset S^3$ (this latter inclusion via stereographic

projection), each planar, so that they are contained in spheres S_i $i = 1, 2$ (respectively), there is a pair of paths p_i of embeddings of the spheres in S^3 which avoids intersecting the graph with infinity and which places them in the great sphere which becomes the x, y-plane under stereographic projection, such that they have the same outermost cycle, with the same orientation. This is an application of Smale's Conjecture (or weaker, just the smooth Schoenflies in dimension 3) [10]. From here induct inward on contiguous components in the complement of the embedded graph in $\mathbb{R}^2$, each time lining up the boundary cycle of the two graphs. The inductive step is an application of Smale's Theorem (or weaker, the smooth Schoenflies Theorem). □

Remark: it is not enough to forbid linking between cycles and knotting of cycles, to guarantee belonging to $Emb_0(X^1, \mathbb{R}^3)$. Figure 5.1 gives a theta graph which is not in the planar component but for which every cycle is the unknot and no two cycles are linked (we might remark this is similar to a Borromean link, however this *ravel* is not detectable on any number of cycles). (Many invariants of these sorts of graph knots can be found in the work of Taniyama). Any valence 3 vertex of a graph embedded in a plane in $\mathbb{R}^3$ can have a neighborhood of this vertex replaced with the knotted half of the given theta graph to yield a linkless and cycle-wise unknotted yet non-planar embedding.

Lemma 5.1.2 designates which cycles are the boundaries of 2-cells, but it does not designate how the 2-cell D should be glued into its boundary cycle, so as to extend to an embedding of X in S^3. In particular, intersecting the image of D with the boundary Σ of a tubular neighborhood of X^1 (i.e., the boundary of a

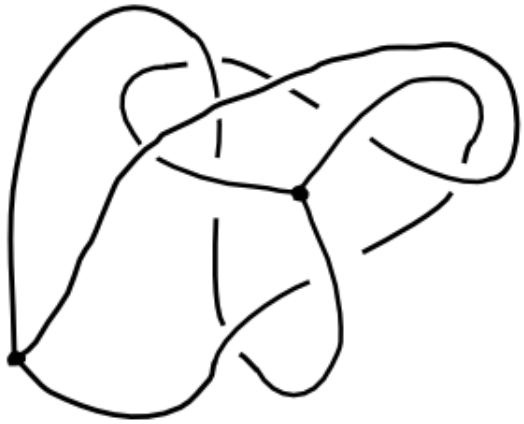

Figure 5.1: A simple example of a graph link which is not detectable on cycles.

handlebody neighborhood retract of X^1) gives us a closed simple curve in Σ. The next lemma says the set of such curves, ranging over all gluings, is contractible.

Lemma 5.1.3. *Given a boundary cycle C in the trivalent polyhedral graph X^1 of the convex polyhedron X, a disk D with $\partial D = C$, an embedding $f : X^1 \to S^3$ in the planar component, and a tubular neighborhood H of $f(X^1)$ with boundary Σ, then the set of elements S of $Emb(S^1, \Sigma)/Aut(S^1)$ resulting from intersecting Σ with an embedding ϕ of D which extends to an embedding of X (agreeing with f on X^1) is contractible.*

Proof. Observe that any such choice of embedding of D results in a simple closed curve in Σ which wraps around edges and vertices along $f(C)$. If Σ' is the boundary of another tubular neighborhood of $f(X^1)$ contained in H, then the deformation retraction from H to $f(X^1)$ induces a homotopy equivalence $\Sigma \simeq \Sigma'$ (viz. x is sent to $\Phi_{t_0}x$ where $t_0 = \min_t \Phi_t(x) \in \Sigma'$). Then decompose Σ' into the closure of

spheres each minus 3 disks union with cylindrical annuli along the edges. Hence $S = \phi(D) \cap \Sigma'$ is decomposed into proper curves in closed annuli and proper curves in the closure of spheres minus 3 disks. Now winding of the curve around a puncture can be pushed back to winding of the curve around the edge, so there is only $Emb(I, D^2 \text{ rel } \partial I) \simeq *$ choice of S at each vertex (see figure 5.2). Two cycles in a 3-connected graph cannot share more than 1 edge, and the gluing curve is parallel to $f(C)$, and unlinked with each of the other cycles in $f(X^1)$, therefore winding about each edge in the annuli must be trivial, since S cannot link with other cycles in $f(X^1)$. This requires one final result which is the configuration space of a closed simple curve representing a homology generator in a surface of genus $k > 1$ is homotopically trivial. □

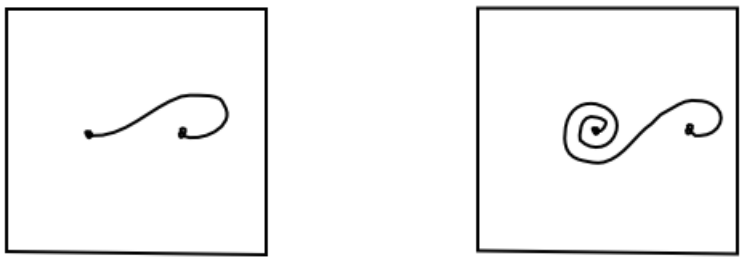

Figure 5.2: The winding about the first vertex in the figure on the right is put onto the edge coincident to it.

Note that it is necessary in this proof that X^1 is polyhedral. The end of the proof relies on the fact that winding about an edge links S with another cycle of $f(X^1)$. Not only is this not the case in non-polyhedral graphs but in fact the previous two lemmata do not hold for non-polyhedral graphs.

For the final step in our theorem we induct on contiguous 2-cells, each time noting that in gluing a 2-cell into the complement of the embedded graph union the 2-cells already glued, we are in fact gluing 2-cells into a handlebody (the complementary handlebody in S^3) relative their boundary, along contractible curves in the handlebody. We find such embeddings are contractible, by noting that a projection of the handlebody to an underlying graph results in a square mapped into a graph relative its boundary, the space of which is contractible as graphs are aspherical. We have shown that the fibration $\rho : Emb_0(X, S^3) \to Emb_0(X^1, S^3)$ has contractible fibers and is therefore a homotopy equivalence. □

In [4] a similar result is proved for arbitrary valence (for a class of graphs which includes all polyhedral graphs except a few overly simple ones) for the PL category. For the remainder of this paper we will stick to trivalent graphs, although the results are expected to hold with only minor technical modifications for graphs with higher valences, based on this PL result of [4].

The structure of $Emb_0(X, S^3)$ as we have defined it (viz. avoiding cusps and flat creases) is easily seen to be a deformation retraction of the space of piecewise differentiable maps from S^2 into S^3 (specifically, use bump functions on partitions of unity parametrized by the curvature near cusps to open the cusps). A similar procedure can be used to smooth out the faces at the edges, and both the edges and faces at the vertices. For a detailed account the reader is referred to [6] as well as the discussion at [13] and the appendix of [10]. Note by Cerf's Theorem [7] the space of S^2 embeddings in S^3 is connected so we can henceforth drop the 0 subscript.

It is not immediately evident that $Emb(X, S^3) \simeq Emb(S^2, S^3)$, as embeddings of X carry with them embeddings of X^1. However, given some $g \in Emb(X^1, S^2)$ each $f \in Emb_0(X^1, S^3)$ factors through g, in a homotopically unique way.

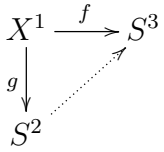

Corollary 5.1.1 relies only on the deformation retraction from Smale's Theorem. If we specify g only up to where a given vertex v of X^1 is sent along with the direction of given edge e coincident to v, call this vector t_e, we've determined g up to isotopy. Hence choosing g to represent the isotopy class sending (v, t_e) to $((1,0,0),(0,0,1))$, say, gives

Lemma 5.1.4. *For X a convex polyhedron with 1-skeleton X^1, $Emb(X, S^3) \simeq Emb(S^2, S^3)$.*

Next we apply the Smale Conjecture, which can be formulated as the more powerful generalization of Cerf's Theorem, $Emb(S^2, S^3) \simeq SO(4)$ (again, see [10]).

It is well known that $SO(4) = SO(3) \times S^3$ (equality denotes homeomorphism here) and easily seen from the split fiber bundle

$$SO(3) \to SO(4) \to S^3$$

where the splitting is due to the action of S^3 on $SO(3)$ (similar to the splitting in 5.1).

The next proposition is near to calculating the homotopy type of $Emb(X^1, \mathbb{R}^3)$, using what we've developed thus far in this chapter.

Proposition 5.1.5.

$$Emb(X^1, \mathbb{R}^3) \times S^3 \simeq \bigvee^n S^1 \times SO(3) \times S^3$$

for the same definitions as in (5.1)

Proof. What remains is to demonstrate a splitting in (5.1) along the minor diagonal. This is achieved by a set parametrization of the handlebody which is the complement of some rigid choice of representative $f(X^1)$ sitting in a great sphere in S^3 with derivative of its lowest ordered edge set in a given direction. The projection to this fiber is the unique SO(4) element which places $f(X^1)$ in the described position. □

In the final theorem of this chapter we remove the S^3 factors from 5.1.5.

Theorem 5.1.6.

$$Emb(X^1, \mathbb{R}^3) \simeq \bigvee^n S^1 \times SO(3)$$

for the same definitions as in (5.1)

Proof. Using Lemmata 5.1.1 through 5.1.4 we assume a certain canonical form for the embedded graph, of which there is a family parametrized up to homotopy by $\bigvee^n S^1 \times SO(3)$. This form has the graph sitting on a sphere S in $\mathbb{R}^3$ with center which is distance D from the origin in $\mathbb{R}^3$and radius $R = \sqrt{D^2 + 4}$.(The relationship between radius and distance ensures that S is the image of a great sphere in S^3 under the stereographic projection $x_i \mapsto 2x_i/(2 - x_4)$.) When $D > 0$

there is a point p in S farthest from the origin. Let κ be a parameter varying from 0 to 1, monotonically, as the distance from p to the embedding of X^1 in $\mathbb{R}^3$, varies from 0 to its maximum, for fixed R. We translate and rescale each embedding moving the center of S along $\kappa_t = (1-t)D + t\kappa D$ and varying the radius along $\sqrt{\kappa_t^2 + 4}$. Now the decomposition becomes apparent: κ_t gives the length along an edge in $\bigvee^n S^1$ (e.g., the planar embeddings in this parametrization correspond to being exactly half way between the vertices in the suspension of $n+1$ points) while the position of S relative to a fixed rigidly embedded S' of the same radius and distance from the origin gives the element of $SO(3)$. $\square$

BIBLIOGRAPHY

[1] Paolo Bellingeri. On automorphisms of surface braid groups. *J. Knot Theory Ramifications*, 17(1):1–11, 2008.

[2] Joan S. Birman. *BRAID GROUPS AND THEIR RELATIONSHIP TO MAPPING CLASS GROUPS*. ProQuest LLC, Ann Arbor, MI, 1968. Thesis (Ph.D.)–New York University.

[3] Joan S. Birman and Tara E. Brendle. Braids: a survey. In *Handbook of knot theory*, pages 19–103. Elsevier B. V., Amsterdam, 2005.

[4] Jeffrey Boyle. Embeddings of 2-dimensional cell complexes in S^3 determined by their 1-skeletons. *Topology Appl.*, 25(3):285–299, 1987.

[5] Tara E. Brendle and Allen Hatcher. Configuration spaces of rings and wickets. *Comment. Math. Helv.*, 88(1):131–162, 2013.

[6] Jean Cerf. Topologie de certains espaces de plongements. *Bull. Soc. Math. France*, 89:227–380, 1961.

[7] Jean Cerf. *Sur les difféomorphismes de la sphère de dimension trois* ($\Gamma_4 = 0$). Lecture Notes in Mathematics, No. 53. Springer-Verlag, Berlin-New York, 1968.

[8] David Michael Dahm. *A GENERALIZATION OF BRAID THEORY*. ProQuest LLC, Ann Arbor, MI, 1962. Thesis (Ph.D.)–Princeton University.

[9] Robert Ghrist. Configuration spaces and braid groups on graphs in robotics. In *Knots, braids, and mapping class groups—papers dedicated to Joan S. Birman (New York, 1998)*, volume 24 of *AMS/IP Stud. Adv. Math.*, pages 29–40. Amer. Math. Soc., Providence, RI, 2001.

[10] Allen Hatcher. A proof of the Smale conjecture, $\mathrm{Diff}(S^3) \simeq \mathrm{O}(4)$. *Ann. of Math. (2)*, 117(3):553–607, 1983.

[11] Allen Hatcher. *Algebraic topology*. Cambridge University Press, Cambridge, 2002.

[12] Youngsik Huh and Choon Bae Jeon. Knots and links in linear embeddings of K_6. *J. Korean Math. Soc.*, 44(3):661–671, 2007.

[13] Robion C. Kirby and Laurence C. Siebenmann. *Foundational essays on topological manifolds, smoothings, and triangulations*. Princeton University Press, Princeton, N.J.; University of Tokyo Press, Tokyo, 1977. With notes by John Milnor and Michael Atiyah, Annals of Mathematics Studies, No. 88.

[14] Riccardo Longoni and Paolo Salvatore. Configuration spaces are not homotopy invariant. *Topology*, 44(2):375–380, 2005.

[15] Per-Olov Löwdin. On the non-orthogonality problem connected with the use of atomic wave functions in the theory of molecules and crystals. *J. Chem. Phys.*, 18:365–375, 1950.

[16] Wilhelm Magnus. Braid groups: a survey. In *Proceedings of the Second International Conference on the Theory of Groups (Australian Nat. Univ., Canberra, 1973)*, pages 463–487. Lecture Notes in Math., Vol. 372. Springer, Berlin, 1974.

[17] Luis Paris. Braid groups and Artin groups. In *Handbook of Teichmüller theory. Vol. II*, volume 13 of *IRMA Lect. Math. Theor. Phys.*, pages 389–451. Eur. Math. Soc., Zürich, 2009.

[18] Luis Paris and Dale Rolfsen. Geometric subgroups of mapping class groups. *J. Reine Angew. Math.*, 521:47–83, 2000.

[19] Johann Radon. Mengen konvexer Körper, die einen gemeinsamen Punkt enthalten. *Math. Ann.*, 83(1-2):113–115, 1921.

[20] J. L. Ramírez Alfonsín. Knots and links in spatial graphs: a survey. *Discrete Math.*, 302(1-3):225–242, 2005.

[21] Neil Robertson, Paul Seymour, and Robin Thomas. A survey of linkless embeddings. In *Graph structure theory (Seattle, WA, 1991)*, volume 147 of *Contemp. Math.*, pages 125–136. Amer. Math. Soc., Providence, RI, 1993.

[22] Lucas Adam Sabalka. *Braid groups on graphs*. ProQuest LLC, Ann Arbor, MI, 2006. Thesis (Ph.D.)–University of Illinois at Urbana-Champaign.

[23] George G. Szpiro. *Poincaré's prize*. Dutton, New York, 2007. The hundred-year quest to solve one of math's greatest puzzles.

[24] Günter M. Ziegler. *Lectures on polytopes*, volume 152 of *Graduate Texts in Mathematics*. Springer-Verlag, New York, 1995.